HHS Public Access

Author manuscript

J Comp Neurol. Author manuscript; available in PMC 2019 January 03.

Published in final edited form as:

J Comp Neurol. 2013 December 15; 521(18): 4318–4338. doi:10.1002/cne.23428.

Alzheimer's Disease Pathology in the Neocortex and Hippocampus of the Western Lowland Gorilla (*Gorilla gorilla gorilla*)

Sylvia E. Perez[1], **Mary Ann Raghanti**[2,3], **Patrick R. Hof**[4], **Lynn Kramer**[5], **Milos D. Ikonomovic**[6,7], **Pascale N. Lacor**[8], **Joseph M. Erwin**[9], **Chet C. Sherwood**[9], and **Elliott J. Mufson**[1,*]

[1]Rush University Medical Center, Chicago, Illinois 60612

[2]Department of Anthropology and School of Biomedical Sciences, Kent State University, Kent, Ohio 44242

[3]Cleveland Metroparks Zoo, Cleveland, Ohio 44109

[4]Fishberg Department of Neuroscience and Friedman Brain Institute, Icahn School of Medicine at Mount Sinai, New York, New York 10029

[5]Dallas Zoo Management, Dallas, Texas 75203

[6]Geriatric Research Education and Clinical Center, VA Pittsburgh Healthcare System, University of Pittsburgh, Pennsylvania 15213

[7]Departments of Neurology and Psychiatry, University of Pittsburgh, Pennsylvania 15213

[8]Neurobiology Department and Cognitive Neurology and Alzheimer's Disease Center, Northwestern University, Evanston, Illinois 60208

[9]Department of Anthropology, The George Washington University, Washington, DC 20052

Abstract

The two major histopathologic hallmarks of Alzheimer's disease (AD) are amyloid beta protein (Aβ) plaques and neurofibrillary tangles (NFT). Aβ pathology is a common feature in the aged nonhuman primate brain, whereas NFT are found almost exclusively in humans. Few studies have examined AD-related pathology in great apes, which are the closest phylogenetic relatives of humans. In the present study, we examined Aβ and tau-like lesions in the neocortex and

*CORRESPONDENCE TO: Elliott J. Mufson, Ph.D., Alla and Solomon Jesmer Chair in Aging, Professor, Neurological Sciences, Rush University Medical Center, 1735 W. Harrison St., Suite 300, Chicago, IL 60612. emufson@rush.edu.

CONFLICT OF INTEREST

The authors report no conflict of interest.

ROLE OF AUTHORS

All authors had full access to all the data in the study and take responsibility for the integrity of the data and the accuracy of the data analysis. Study concept and design: E.J. Mufson, S.E. Perez, and M.A. Raghanti. Acquisition of data: S.E. Perez, E.J. Mufson, and M.A. Raghanti. Analysis and interpretation of data: E.J. Mufson and S.E. Perez. Drafting of the article: S.E. Perez and E.J. Mufson. Critical revision of the article for important intellectual content: L. Kramer, M. Ikonomovic, J.M. Erwin, P. Lacor, C.C. Sherwood, P.R. Hof, and M.A. Raghanti. Obtained funding: E.J. Mufson, C.C. Sherwood, P.R. Hof. Facilitation of access to specimens: P.R. Hof, C.C. Sherwood, M.A. Raghanti, J.M. Erwin. Administrative, technical, and material support: M. Nadeem, C. Stimpson, L. Shao, and S. Shoaga. Study supervision: E.J. Mufson.

hippocampus of aged male and female western lowland gorillas using immunohistochemistry and histochemistry. Analysis revealed an age-related increase in Aβ-immunoreactive plaques and vasculature in the gorilla brain. Aβ plaques were more abundant in the neocortex and hippocampus of females, whereas Aβ-positive blood vessels were more widespread in male gorillas. Plaques were also Aβ40-, Aβ42-, and Aβ oligomer-immunoreactive, but only weakly thioflavine S- or 6-CN-PiB-positive in both sexes, indicative of the less fibrillar (diffuse) nature of Aβ plaques in gorillas. Although phosphorylated neurofilament immunostaining revealed a few dystrophic neurites and neurons, choline acetyltransferase-immunoreactive fibers were not dystrophic. Neurons stained for the tau marker Alz50 were found in the neocortex and hippocampus of gorillas at all ages. Occasional Alz50-, MC1-, and AT8-immunoreactive astrocyte and oligodendrocyte coiled bodies and neuritic clusters were seen in the neocortex and hippocampus of the oldest gorillas. This study demonstrates the spontaneous presence of both Aβ plaques and tau-like lesions in the neocortex and hippocampus in old male and female western lowland gorillas, placing this species at relevance in the context of AD research.

Keywords

aging; amyloid; brain; evolution; great ape; mammals; pathology; tau

Amyloid beta protein (Aβ) deposits (or senile plaques), Aβ angiopathy, and neurofibrillary tangles (NFT) consisting of hyperphosphorylated tau aggregates are common pathological features in the brains of healthy aged humans and in Alzheimer's disease (AD) (Braak and Braak, 1991; Bouras et al., 1994). In humans, Aβ plaques are mainly composed of a 42-amino acid Aβ species (Aβ42), whereas 40-amino acid (Aβ40) peptides are found mostly in the cerebral vasculature (Attems et al., 2004). These peptides are derived from the amyloid precursor protein (APP) through the concerted proteolysis action of β- and γ-secretase. Aβ42 has a high propensity to aggregate into insoluble fibrils and is more toxic than Aβ40 (Younkin, 1998; Selkoe, 2001). AD is characterized by the appearance of neuritic plaques (mature plaques) with a central amyloid core and dystrophic neurites and diffuse Aβ plaques with an amorphous appearance and lacking dense fibrillar structures. The amyloid cascade hypothesis of AD proposes Aβ production as a necessary precondition for the development of tau-containing NFTs (Selkoe, 2000). Tau is a microtubule-associated protein that is abnormally hyper-phosphorylated and self-assembles into paired-helical filaments (PHF) in AD and other tauopathies. Clinical pathological studies have demonstrated that, unlike diffuse plaques, neuritic plaques as well as the amount and distribution of NFT correlate with cognitive decline in AD (Arriagada et al., 1992; Nagy et al., 1995; Gomez-Isla et al., 1996; Giannakopoulos et al., 2003).

The sporadic presence of parenchymal and vascular Aβ deposits is not exclusive to aged humans and have been reported in the brain of aged nonprimate mammals as well as nonhuman primates (strepsirrhines, monkeys, and apes), suggesting that age-related Aβ plaque deposits occur in most mammalian species. Mainly Aβ40 and/or Aβ42 diffuse plaques have been described in the brain of aged nonprimate mammals including camels (Nakamura et al., 1995), polar bears (Tekirian et al., 1996), wolverines (Roertgen et al., 1996), dogs (Tekirian et al., 1996), and cats (Brellou et al., 2005). In contrast, the brains of

several New and Old World monkeys, such as marmosets (Geula et al., 2002), rhesus monkeys (Martin et al., 1991; Mufson et al., 1994; Poduri et al., 1994; Gearing et al., 1996), long-tailed macaques (Kimura et al., 2003), Caribbean vervets (Lemere et al., 2004), squirrel monkeys (Walker et al., 1987), and cotton-top tamarins (Lemere et al., 2008) display mainly Aβ neuritic plaques and Aβ vascular deposits similar to those seen in humans, indicative of similar mechanisms involved in Aβ processing between monkeys and humans. However, the absence of the classic NFT pathology in monkeys (Hartig et al., 2000; Schultz et al., 2000) despite amyloid plaque deposition suggests the existence of differential molecular machinery involved in NFT formation between monkeys and humans.

While numerous studies exploring the presence of AD-like pathology have been carried out in aged New and Old World monkeys, only a few studies have been performed in apes (Gearing et al., 1996, 1997; Kimura et al., 2001; Rosen et al., 2008). As great apes and humans share numerous anatomical and physiological similarities due to their close genetic ancestry, the knowledge of interspecies differences in AD-like pathology could provide clues to the mechanisms underlying AD pathology in humans. Among the great apes, chimpanzees and bonobos display the closest phylogenetic relationship to humans, followed by gorillas and orangutans (Scally et al., 2012). Although prior studies have revealed diffuse plaques and vascular amyloid in the aged chimpanzee (Gearing et al., 1996) and orangutan (Gearing et al., 1997) brain, reports of tau pathology are restricted to a single old chimpanzee with a large vascular lesion (Rosen et al., 2008). With the exception of data from an aged western lowland gorilla showing only plaque pathology (Kimura et al., 2001), there is a paucity of literature examining amyloid and tau pathology in gorillas. Therefore, in this special issue of *The Journal of Comparative Neurology* dedicated to the memory of Gary Van Hoesen, we present an analysis of AD-like pathology in the neocortex and hippocampus in aged male and female western lowland gorillas, brain regions to which he applied his neuroanatomical expertise to define their neural connectivity and involvement in AD.

MATERIALS AND METHODS

Subjects

The study sample included adult western lowland gorillas (*Gorilla gorilla gorilla)* that had been housed at American Zoos and Aquariums (AZA)-accredited facilities within the United States and were maintained in accordance with each institution's animal care and use guidelines. All individuals died of natural causes and brains were obtained through the Great Ape Aging Project. All specimens are "on loan" to the "Great Ape Aging Project," which is authorized to share access with scientists for research that amplifies knowledge of great apes. The zoological institutions indicated that overt cognitive decline was not noted for any of the gorillas that were included in this study. However, none of the individuals participated in formal cognitive testing. Frontal cortex was obtained from four males (22 to 49 years) and three females (32, 50, and 55 years old) and hippocampus materials from two males (13 and 42 years old) and four females (32 to 55 years) (Table 1).

The western lowland gorilla represents one of the closest living relatives of humans, demonstrated by the recent sequencing of the gorilla genome (Scally et al., 2012), having

shared a common ancestor with humans ~9-20 million years ago (Langergraber et al., 2012). In the wild, western lowland gorillas inhabit the tropical forests of Cameroon, Central African Republic, Gabon, Democratic Republic of Congo, and Equatorial Guinea, with a primarily herbaceous and frugivorous diet (Doran et al., 2002). The maximum lifespan of wild western lowland gorillas ranges from 35 to 40 years (Bronikowski et al., 2011), whereas captive individuals have exceeded 50 years.

Tissue preparation

Brains were immersion fixed in a 4% paraformaldehyde phosphate buffered (PB, pH 7.4) solution for a minimum of 7 to 10 days and then cryoprotected in graded series of sucrose solutions at 4°C. Blocks containing the frontal cortex and the hippocampus were cut in the coronal plane at 40 μm thickness on a freezing-sliding microtome and stored in a solution containing 30% glycerin, 30% ethylene glycol, in 0.1 M phosphate buffer at −20°C until processing for immunohistochemistry and histochemistry.

Antibodies

Table 2 describes the antibodies used in the present study including: 6E10, a mouse IgG1 antibody raised against amino acid residue 1–16 (DAEFRHDS-GYEVHHQK) of Aβ, with an epitope at residues 3–8 (Kim et al., 1988), which recognizes Aβ isoforms and its precursor APP protein (1:1,000 dilution, Covance, Princeton, NJ); 4G8, a monoclonal antibody recognizing amino acid residues 17–24 (LVFFAEDV) of Aβ with the epitope lying within amino acids 18–22 (1:1,000, Covance); MOAB-2 (clone 6C3), a mouse IgG_{2B} antibody raised against human Aβ, with an epitope at residues 1–6 (DAEFRH) and recognizing Aβ40 and Aβ42 (Youmans et al., 2012) (1:600, gift from Dr. Mary Jo LaDu, University of Illinois at Chicago, IL); an Aβ40 rabbit IgG antibody raised against a 7-amino acid (LMVGGVV) from the C-terminus of human Aβ40 (1:100, Millipore, Billerica, MA); an Aβ42 rabbit IgG antibody raised against the C-terminus of human Aβ A4 protein which does not crossreact with Aβ40 (1:100, Invitrogen, Grand Island, NY); NU4, an antibody raised against Aβ-derived diffusible ligands that preferentially binds Aβ oligomers over monomers (Lambert et al., 2007) (1:2,000, gift from Dr. William Klein, Northwestern University, Evanston, IL); Alz50, a mouse IgM raised against amino acid residues 5–15 (QEFEVMEDHA) and 312–322 (GSTENLKHQPGG) of human PHF-tau (Carmel et al., 1996; Jicha et al., 1997) and recognizing an early stage conformational tau epitope that marks neurons undergoing early degenerative events associated with NFT formation (Wolozin et al., 1986) (1:500 dilution, gift from Dr. Peter Davies, Albert Einstein School of Medicine, NY); MC1, a mouse IgG that recognizes an early stage of conformational tau (Jicha et al., 1997) (1:200, gift from Dr. Peter Davies, Albert Einstein School of Medicine, NY); AT8, a mouse IgG1 antibody raised against partially purified human PHF-Tau, with an epitope at residues phosphoserine202/phosphothreo- nine205 (Goedert et al., 1995a; Rosen et al., 2008) that recognizes a tau phosphorylated isoform (1:000 dilution, ThermoFisher, Waltham, MA); Anti-200 kDa + 160 kDa phosphorylated neurofilament proteins SMI-34 antibody mouse IgG1 raised against homogenized hypothalamus recovered from Fischer 344 rats and recognizing a phosphorylated epitope in extensively phosphorylated 200 kDa and 160 kDa neurofilaments proteins (Vickers et al., 1994) (1:1,000, Abcam, Cambridge, MA); Neuro-Chrom Pan Neuronal Marker/Alexa488 conjugated, a rabbit IgG antibody raised

against whole neuron and specific revealed neurofilament in axons, dendrites and neuronal somas (1:1,000, Millipore); an anti-choline acetyltransferase (ChAT) goat IgG antibody raised against human placental ChAT (Raghanti et al., 2008) (1:1,000 dilution, Millipore) that specifically recognizes cholinergic neurons (Mufson et al., 1989); and an anti-glial fibrillary acid protein (GFAP) rabbit IgG raised against GFAP isolated from cow spinal cord that specifically detects astrocytes (Gaillard et al., 2008) (1:400, Dako, Denmark). Antibody specificity was determined by western blot 6E10 (Covance), 4G8 (Covance), MOAB-2 (Youmans et al., 2012), Aβ40 (Millipore), Aβ42 (Invitrogen), AT8 (Goedert et al., 1995a), Alz50 (Carmel et al., 1996; Jicha et al., 1997), and MC1 (Jicha et al., 1999), ChAT (Mufson et al., 1989), SMI-34 (Vickers et al., 1994), and GFAP (Gaillard et al., 2008).

Immunohistochemistry and immunofluorescence

Neocortex and hippocampus free-floating sections were singly stained for the following antibodies: 6E10 (APP/Aβ), Alz50, and AT8. Prior to staining, sections were washed 3 × 10 minutes in phosphate buffer and 3 × 10 minutes in Tris-buffered saline (TBS, pH 7.4) to remove cryoprotectant before a 20-minute incubation in 0.1 M sodium metaperiodate (Sigma, St. Louis, MO) in TBS to inactivate endogenous peroxidase activity. Tissue was then permeabilized 3 × 10 minutes in TBS containing 0.25% Triton-X (ThermoFisher) and blocked in the same solution containing 3% goat serum for 1 hour. Sections were incubated with appropriate antibody dilutions overnight on an orbital shaker at 45 rpm at room temperature in 0.25% Triton X-100, 1% goat serum solution. The next day, tissue was washed 3 × 10 minutes in TBS containing 1% goat serum prior to incubation with appropriate secondary antibody (Table 2) at a 1:200 dilution for 1 hour. Following 3 × 10 minutes washes in TBS, sections were incubated using the Vectastain ABC kit (Vector Laboratories, Burlingame, CA) in TBS for 1 hour. Tissue was then rinsed 3 × 10 minutes in 0.2 M sodium acetate, 1.0 M imidazole buffer, pH 7.4, and developed in acetate-imidazole buffer containing 0.05% 3,3′-diaminobenzidine tetrahy-drochloride (DAB, Sigma) with or without nickel intensification (1% nickel sulfate). The reaction was terminated in acetate-imidazole buffer, tissue mounted on glass slides, dehydrated through graded alcohols (70–95–100%, 3 × 5 minutes), cleared in xylene (3 × 5 minutes), and coverslipped using DPX (Biochemica Fluka, Buchs, Switzerland). Some sections were also singly stained with anti-Aβ40 and anti-Aβ42 antibodies (Table 2) using the protocol described above. Staining with antibodies MOAB-2 and SMI-34 (Table 2) was performed on sections mounted on charged slides that were pretreated for antigen-retrieval with 88% formic acid for 6 minutes or boiled in 0.01 M citric acid (pH 8.5) for 20 minutes, respectively. Selected sections were Nissl-counterstained with cresyl violet for cytoarchitectural evaluation. In addition, as a positive control for each antibody, we stained cortical sections from human AD cases known to have extensive amyloid plaque and NFT pathology (Braak scores V-VI). Neo- cortical and hippocampal nomenclature was based on the cytoarchitecture of the human and monkey brain (Brodmann, 1909; Rosene and Van Hoesen, 1987).

Brain sections also were double-immunostained for APP/Aβ and Alz50, and APP/Aβ and ChAT. After finishing the standard protocol for single ChAT and Alz50 immunolabeling using nickel intensification (Perez et al., 2004, 2012a), sections were washed with TBS and incubated with APP/Aβ (6E10) antibody for 24 hours in a medium containing TBS 0.25%

Triton X-100 and 1% goat normal serum. The following day, sections were incubated with biotinylated goat antimouse secondary antibody (Vector Laboratories) and visualized with the chromogen DAB (brown) without nickel intensification or were incubated using the Vector NovaRed substrate kid (red). This dual staining resulted in an easily identifiable two-colored profile: dark blue/black for Alz50 and ChAT profiles and brown or red for APP/Aβ-positive plaques/blood vessels (Perez et al., 2011, 2012a). Brightfield images were acquired using a Nikon Eclipse 80i microscope.

Additional sections were double-labeled for immunofluorescence with antibodies directed against APP/Aβ (1:100; 6E10) and GFAP (1:400). Fluorescence signals were revealed using Cy2- (1:200) and Cy3- (1:300) conjugated antimouse and -rabbit IgGs (Jackson Immunoresearch, West Grove, PA) for APP/Aβ and GFAP, respectively, and images were analyzed with the aid of a Zeiss Axioplan 2 (Zeiss, Thornwood, NY). Cortical sections were single, double, or triple-stained with antibodies against Aβ oligomers (NU4, 1:2000), APP/Aβ (4G8, 1:1000), and/or a neuronal marker (1:1,000) as previously described (Lacor et al., 2004; Lambert et al., 2007). After incubation for 3 days at 4°C under gentle shaking, sections were washed and incubated with secondary Alexa Fluor488-, 555-, or 633-conjugated anti-IgG (1:500, Molecular Probes, Eugene, OR) for 2 hours at room temperature. Sections were mounted with ProLong Gold Antifade Reagent with DAPI (Life Technology, Carlsbad, CA). These images were visualized and acquired with the aid of a Leica confocal SP5 microscope equipped with a diode (405 nm), and Ar, Green HeNe, and Red HeNe lasers.

Histofluorescence p

Several sections were stained with thioflavine S, X-34, and 6-CN-PiB to examine the fibrillar nature of plaques. Sections processed for thioflavine S were air-dried, defatted with chloroform-ethanol (1:1), followed by rehydration through a graded series of ethanol (70–100%). Sections were stained with 0.1% aqueous thioflavine S (Sigma) for 10 minutes at room temperature and differentiated in 80% ethanol. After several distilled water rinses, slides were coverslipped with an aqueous mounting medium (Gel-Mount; Biomeda, Foster City, CA). Sections labeled for 6-CN-PiB were slide-mounted and incubated in a 10 mM 6-CN-PiB solution for 45 minutes. Slides were dipped three times in phosphate buffer (PB; 0.1 M), followed by a 1-minute differentiation in a solution containing 132.9 mM NaCl, 8.7 mM K_2HPO_4, and 1.5 mM KH_2PO_4 (pH 7.4). Slide-mounted tissue sections were also processed for X-34 (0.04 g/l) as previously reported (Ikonomovic et al., 2006). X-34 is a highly fluorescent derivative of Congo Red, which detects the full spectrum of amyloid pathology including neurofibrillary tangles and Aβ plaques, with greater sensitivity than thioflavine S (Styren et al., 2000; Ikonomovic et al., 2006). Tissue sections were coverslipped with Fluoromount (Electron Microscopy Services, Hatfield, PA) and analyzed with the aid of a Zeiss Axioplan 2 microscope. Histofluorescent and immunohistochemical photomicrographs were stored on a computer and brightness/contrast were manipulated using Adobe Photoshop (v. 7, San Jose, CA).

Mapping of APP/Aβ plaques and Alz50-immunoreactive profiles

Neocortical and hippocampal distribution of APP/Aβ-immunoreactive (ir) plaques and Alz50-ir profiles from the 55-year-old female gorilla were charted using Neurolucida 8 (MBF Bioscience, Williston, VT) with the aid of Nikon Optiphot-2 microscope. Sections were outlined at 1× magnification, and distribution/counts of plaques and Alz50-ir profiles in the cortex and hippocampus was performed manually at 10× magnification and fiduciary landmarks were used to prevent repeat counting of labeled profiles (Perez et al., 2012b).

Quantification of Aβ optical density and plaque load and size

Quantification of the relative optical density (OD) measurements of cortical Aβ40 and Aβ42 immunoreactivity was performed using the densitometry software program Image 1.60 (Scion 1.6, Frederick, MD). Plaques were measured in two adjacent sections from the frontal cortex of a 55-year-old female gorilla. Seventy randomly chosen plaques per section were manually outlined and area/OD were automatically measured and analyzed in gray-scale images under 10× objective. Thirty ODs from regions of the cortex devoid of Aβ40 or Aβ42 immunostaining were measured, averaged, and subtracted from the final Aβ40 and Aβ42 OD values. Previous studies have shown that OD measurements reflect changes in protein expression, which parallel those obtained using a biochemical protein assay (Mufson et al., 1997). Plaque load, measured as percent area occupied for Aβ40 and Aβ42-ir plaques in adjacent cortical sections or between cortical areas, were evaluated with the aid of a Nikon Eclipse 80i using NIS-element software (Nikon, Melville, NY). Individual cortical plaque area contained within 6 mm^2 of cortex was measured in six matching regions at the level shown in Figure 2A. Each plaque was manually outlined at 4× magnification and area was automatically measured.

Statistical analysis

Data obtained from Aβ OD measurements, plaque load, and plaque size, were evaluated using a *t*-test (Sigma Stat 3.5; Systat Software, San Jose, CA). Correlations were performed with a Spearman test. Statistical level of significance was set at $\alpha = 0.05$ (twotailed). The data were graphically represented using the means and standard error of the mean (SEM) (Sigma Plot 10.0; Systat Software).

RESULTS

APP/Aβ plaque and vascular immunostaining in the frontal cortex

APP/Aβ-ir plaques and blood vessels were distributed within each prefrontal cortex Brodmann areas 6, 8, 9, 45, 46, anterior cingulate areas 24 and 25, and orbitofrontal areas 13, 14, and 47 in aged male (42, 43, and 49 years old) and female (50 and 55 years old) gorillas. Notably, aged females displayed more APP/Aβ-ir plaques than male gorillas, whereas the males contained more vascular staining (Fig. 1A–N). APP/Aβ-ir plaques were distributed throughout all of the layers in each of the cortical regions examined in the 50- and 55- year-old female gorillas (Figs. 1A,B and 2). These regions also contained APP/Aβ-ir meningeal arteries, arterioles, and capillaries (Fig. 1C–G). Qualitatively many more APP/Aβ-ir plaques were observed in the cortex of the 55-year-old compared to a 50-year-old

female gorilla (Fig. 1A,B). In fact, a semiquantitative plaque load analysis of cortical areas 8 and 44 revealed that the percentage of area occupied by plaques in the 55-year-old was 2.5 times higher than in the 50-year-old gorilla. Interestingly, we found that the plaque APP/Aβ intensity and size displayed a laminar gradient in the cortical areas examined in the oldest gorilla (Fig. 1B). For example, strongly APP/Aβ-ir compact plaques were located primarily within the supragranular layers (I-III) compared to paler and larger stained plaques mostly within the infragranular (V-VI) layers as well as in the interface between white and gray matter (Fig. 1B).

In general, discrete small plaques (Fig. 1H,I) and large irregularly shaped plaques (Fig. 1J) lacking a perceptible central core, a feature of neuritic plaques, were found in all cortical regions in both older female gorillas. Plaque size, measured as plaque area (μm^2), ranged between 200 (15 μm diameter) to 6,000 μm^2 (87 μm diameter) in the 50-year-old gorilla, whereas in the 55-year-old gorilla the area of a plaque reached 27,000 μm^2 (185 μm diameter), 4 times the maximum size seen in the 50-year-old female gorilla. APP/Aβ-ir plaques were also found in clusters (Fig. 1K) or associated with blood vessels (Fig. 1E,F). In some small blood vessels, mainly arterioles and capillaries, Aβ immunore-activity appeared as perivascular leaks (Fig. 1E) or gave the appearance of collapsing upon a blood vessel (Fig. 1E,G). In the 22-year-old male there were virtually no APP/Aβ-ir plaques or blood vessels in the cortical areas examined. In contrast, numerous APP/Aβ-ir meningeal arteries, arterioles, and capillaries as well as a few positive plaques throughout the neocortex, which varied between 100 μm^2 (10 μm in diameter) to 1,500 μm^2 (50 μm in diameter) in the 42, 43, and 49-year-old male gorillas (Fig. 1L–Q). Interestingly, a 42-year-old male gorilla showed many more APP/Aβ-ir vascular profiles than either the 43- and 49-year-old male gorillas and contained the largest plaques (area of 4,000 μm^2).

APP/Aβ plaque and vascular immunostaining in the hippocampus

There were no APP/Aβ-ir plaques or blood vessels in the hippocampus of the youngest female (32 and 35 years old) and male (13 years old) gorillas. The hippocampus of the 55-year-old female gorilla displayed more APP/Aβ pathology than either the 50-year-old female or the 42-year-old male gorillas (Fig. 3A–C). Interestingly, the pattern of plaque distribution in the hippocampus of the 42-year-old male as well as the 50- and 55-year-old female gorillas were similar. APP/Aβ-ir plaques and blood vessels (mainly arterioles and capillaries) were mainly seen in the hippocampal CA1 pyramidal layer and molecular layer of the dentate gyrus (Fig. 3B–D), as well as the subicular formation as shown in the drawings obtained from the older female gorilla (Fig. 3G,H). APP/Aβ-ir blood vessels were confined mainly to the CA4 (hilar portion of the CA3) (Fig. 3A–C), while only a few Aβ-ir plaques and capillaries were seen in the hippocampal CA3 and CA2 fields (Fig. 3G,H). Additionally, in the oldest female gorilla APP/Aβ-ir plaques were seen also in the granule cell layer of the dentate gyrus (Fig. 3C). Scattered labeled plaques and capillaries were found mainly in the pyramidal cell layer of the subiculum and throughout the entorhinal cortex (Fig. 3E) and parahippocampal gyrus (Fig. 3F). In general, the hippocampus of male and female gorillas exhibited small amorphous APP/Aβ-ir plaques (Fig. 3B), and immunopositive capillaries were also surrounded by perivascular Aβ or collapsed capillary lumen (Fig. 3B), similar to that seen in the cortex (Fig. 1G). Plaque sizes in the

hippocampus varied between 100 μm^2 (10 μm in diameter) to 1500 μm^2 (50 μm in diameter).

Aβ subtype pathology in the neocortex and hippocampus

To further examine Aβ subtype pathology, we stained neocortical and hippocampal sections adjacent to those previously shown to contain extensive APP/Aβ-ir plaques and vasculature, with antibodies that detect both Aβ40 and Aβ42/43 (MOAB−2) or individually for Aβ40, Aβ42, and oligomeric Aβ (NU4) (Lacor et al., 2004; Lambert et al., 2007). The morphology and topographic distribution of MOAB-2 labeled plaques and vessels in the 42-year-old male and 55-year-old female gorillas (Fig. 4A–E) were comparable to those stained for 6E10 (APP/Aβ) (Fig. 1A,B), indicating that the main amylodogenic component in gorilla plaques is Aβ.

Although Aβ40 and Aβ42 immunoreactivity were seen in plaques and blood vessels in the neocortex and hippocampus, differences in the distribution of plaques immunoreactive for these markers were observed in some of the neocortical areas examined (Fig. 4F–H). For instance, area 24 displayed widespread Aβ42- positive plaques in all layers compared to Aβ40 (Fig. 4F,G), and Aβ40-ir plaques seemed to be more strongly labeled than Aβ42-ir plaques (Fig. 4I,J). On the other hand, oligomeric Aβ immunoreactivity was found in all APP/Aβ-ir plaques (Fig. 4L,N,O) in sections examined from the oldest female gorilla as well as in human AD frontal cortex (Fig. 4M,P,Q).

Semiquantitative analysis of plaque load, plaque size, and OD measurements for Aβ40 and Aβ42 immunoreactivity were performed in the frontal cortex from the 55-year-old female gorilla at the level shown in Figure 2A. Although plaque load ranged from 0.7 to 3.5% for Aβ40 and from 1.07 and 2.8% for Aβ42 (Fig. 5A), no significant differences were found between Aβ40 and Aβ42. OD measurement revealed that Aβ40-positive plaques were significantly more immunoreactive than Aβ42 plaques (Fig. 5B, *t*-test, $P < 0.001$). Plaque size correlated negatively with OD measurements for Aβ40 immunoreactivity, suggesting that OD measurements for Aβ40-ir tend to decrease with increased plaque size (Fig. 5C; $r = -0.335$, $P = 0.0471$).

Thioflavine S, X-34, and 6-CN-PiB profiles in the neocortex and hippocampus

Thioflavine S, X-34, and 6-CN-PiB staining, which reveal the presence of β-pleated sheet structures, were performed to establish the extent of Aβ fibrils (conformation state) in plaques and blood vessels in the gorilla brain. In neocortical and hippocampal sections, blood vessels showed stronger thioflavine S fluorescence compared to plaques (Fig. 6A–C). Both plaques and vascular amyloid were prominently labeled with the panamyloid marker X-34, in both gorilla and human AD tissue (Fig. 6D,E,H). In addition, X-34 did not reveal dystrophic neurites surrounding amyloid deposits, NFT, or neuropil threads in the gorilla compared to AD (Fig. 6D,H). In contrast, vascular deposits showed stronger immunoreactivity than plaques with 6-CN-PiB in the gorilla (Fig. 6F,G), whereas cortical plaques and vessels displayed stronger reactivity in AD (Fig. 6I). Together these results suggested that the majority of Aβ peptides in gorilla do not display a dense Aβ-pleated sheet

conformation, a feature of classic neuritic/compact plaques, whereas fibrillar Aβ is more abundant in blood vessels.

Absence of dystrophic neurites surrounding plaques in neocortex and hippocampus

To evaluate whether plaques were associated with dystrophic neurites, cortical and hippocampal sections were singly stained with SMI-34, an antibody that reveals the presence of heavy and medium phosphorylated neurofilament proteins, as well as doubly stained with ChAT and 6E10 antibodies, or triple stained for oligomeric NU4, 4G8 (APP/Aβ), and neurofilament proteins. In general, there was an absence of SMI-34-ir cells and dystrophic processes in the neocortex and hippocampus in all male and most female gorillas (Fig. 7A–L). On the other hand, a few sporadic SMI-34-ir cells and clusters of swollen neurites were observed in the cortex (Fig. 7B–G) and hippocampus of the oldest female gorilla (Fig. 7H,I,K,L). In contrast, neocortical tissue from a human AD subject used as positive control displayed numerous SMI-34 positive NFTs (Fig. 7M,N), neuropil threads (Fig. 7N), and swollen neurites within plaques (Fig. 7O). Although extensive ChAT-ir cortical and hippocampal fibers were observed in close association with APP/Aβ-ir amyloid plaques and vessels in the gorilla brains, there were no signs of morphological alterations (Fig. 7P–R). Likewise, neurofilament proteins did not show signs of dystrophy in the proximity to oligomeric NU4-ir plaques (Fig. 7S–V).

Astrocytosis in neocortex and hippocampus

To investigate whether amyloid positive plaques and blood vessels were associated with astroglia, neocortical and hippocampal sections were doubly immunostained for GFAP and APP/Aβ. APP/Aβ-ir plaques and blood vessels were surrounded by GFAP-positive astrocytes, but qualitatively capillaries appeared to display stronger GFAP immunoreactivity compared to plaques (Fig. 8).

Tau-like pathology in the neocortex and hippocampus

To examine the presence of alterations in tau, neocortical and hippocampal sections were stained with antibodies against Alz50 and MC1 early tau conformational epitopes as well as AT8, which recognize an earlier phosphorylated form of tau. A rostral-to-caudal schematic representation of the distribution of neocortical and hippocampal Alz50-ir profiles seen in the oldest female gorilla is depicted in Figures 2 and 3, respectively. Scattered, fusiform-shaped Alz50-ir cells were found in the neocortex and hippocampus in both male (Fig. 9A–F) and female (Fig. 9G–J) gorillas at each age examined. Alz50 immunostaining appeared as fine granules within somata and processes in the neocortex and hippocampus (Fig. 9A–J). These neurons, together with fine-beaded Alz50-ir fibers, were distributed principally in supragranular cortical layers in each gorilla (Fig. 9D), as well as a few clusters of Alz50-ir neurites in the neocortex of the aged individuals (Fig. 9F). Hippocampal Alz50-ir neurons with similar morphology to those observed in the cortical areas were mostly seen in the subiculum (Fig. 9I), a few in the hippocampal CA1-CA3 fields, and virtually none in the dentate gyrus. Dual immunostaining revealed normal-appearing Alz50-ir neurons in close association to APP/Aβ plaques (Fig. 9J).

In addition, scattered Alz50- (Fig. 9K–N) and MC1-ir (Fig. 9O–Q) structures resembling astrocytic or oligodendrocyte-coiled bodies (Schultz et al., 2000) were occasionally seen at the interface of white and gray matter or within the neocortex in the oldest gorillas (Fig. 9K–Q). AT8-labeled astrocytes, neurons, as well as cluster of neurites were seen throughout the neocortex (Fig. 9S,T) and hippocampus (Fig. 9U,V). However, neither typical AD flame-shaped NFTs (Fig. 9R,W) nor tau-ir neuropil threads (Fig. 9W) were found in the neocortex or hippocampus at any age examined.

DISCUSSION

Although Aβ plaques, Aβ angiopathy, and NFTs are pathological hallmarks of human AD, Aβ-containing plaques and blood vessels are not exclusive to humans and have been described in several other mammalian species (Brellou et al., 2005; Roertgen et al., 1996; Tekirian et al., 1996), including a large number of non-human primate species (Walker et al., 1987, 1990; Martin et al., 1991; Mufson et al., 1994; Poduri et al., 1994; Gearing et al., 1996; Kimura et al., 2001; Geula et al., 2002; Lemere et al., 2004; Bons et al., 2006), and some great apes (Gearing et al., 1996, 1997; Kimura et al., 2001). In contrast, NFT pathology, which is characteristic of human tauopathies, has rarely been described in the nonhuman primate brain with the exception of a single aged chimpanzee (Rosen et al., 2008), despite anatomical and physiological similarities across species (Huxley, 1863). The gorilla genome shows 96% sequence homology with humans and their lifespan is among the longest for a nonhuman primate, making it an excellent species in which to investigate the onset of AD-like pathology in the neocortex and hippocampus. Nonetheless, maximum potential longevity in humans is much longer than gorillas, whose lifespan in captivity ranges from 40 to 55 years.

In the present study, we report the first evidence that Aβ pathology increases with age in the brain of the male and female western lowland gorilla. Aβ-positive plaques and blood vessels were seen in the neocortex and/or hippocampus of aged male (42, 43, and 49 years old) and female (50 and 55 years old), while these deposits were not seen in the youngest males (13 and 22 years old) and only a few plaques were seen in the cortex of a 32-year-old female gorilla. Old male gorillas displayed comparatively fewer Aβ plaques than Aβ vessels, whereas aged female gorillas showed much more cortical and hippocampal parenchymal plaque deposition, suggesting sex differences in Aβ production similar to that described in transgenic mouse models of AD, which overexpress Aβ (Hirata-Fukae et al., 2008; Overk et al., 2012). Our findings differ from a previous report showing Aβ-containing plaques but not immunoreactive blood vessels in a male 44-year-old western lowland gorilla (Kimura et al., 2001), a discrepancy that may be due to methodological differences or to the normal interindividual variation in the degree to which aging primates are affected by Aβ deposition. Other aged great apes, such as the common chimpanzees (*Pan troglodytes*) and Borneo orangutans (*Pongo pygmaeus),* also display cortical Aβ plaques, but only the chimpanzee has shown widespread Aβ vascular deposition in the neocortex and hippocampus (Gearing et al., 1997). In humans, Aβ deposition in cerebral blood vessels is frequent in patients with vascular cognitive impairment, AD, and Down syndrome (Rensink et al., 2003; Attems et al.,2005), suggesting a strong association between parenchymal and vascular Aβ deposition across all hominids, perhaps a reflection of cerebrovascular

deterioration or impaired Aβ clearance with age. Parenchymal and vascular deposits have been described in the brain of aged monkeys (Poduri et al., 1994; Mufson et al., 1994; Gearing et al., 1996, 2003; Schultz et al., 2000; Elfenbein et al., 2007; Atsalis and Margulis, 2008) as well as in other nonprimate mammals (Nakamura et al., 1995; Roertgen et al., 1996; Tekirian et al., 1996; Brellou et al., 2005). It is noteworthy that the maximum lifespan of gorillas in the wild ranges from 35 to 40 years (Bronikowski et al., 2011), whereas in captivity it can reach upwards of 50 years (Atsalis and Margulis, 2008). In this study, the oldest gorilla displayed the highest amount of plaques and is the oldest reported gorilla to have died in captivity, suggesting that age is a major risk factor for the development of Aβ pathology in gorillas, similar to human AD.

The presence of Aβ deposits in the microvasculature or cerebral amyloid angiopathy (CAA) was a common feature in the neocortex and hippocampus in all aged gorillas examined. Aβ-positive blood vessels displayed different sizes indicative of meningeal and parenchymal arteries, arterioles, and capillaries. We also observed numerous capillaries in close association with plaques showing perivascular Aβ leakage and occluded Aβ accumulation resembling dyshoric angiopathy as described in capillaries in CAA and AD (Clifford et al., 2008; Thal et al., 2008b). CAA is characterized by extracellular deposition of Aβ in the walls of cerebral and leptomeningeal vessels and is a commonly seen feature in AD. The topographic distribution of Aβ blood vessels in the neocortex and hippocampal formation in the oldest female gorilla is reminiscent of the hierarchical stage 3 of CAA in humans (Olichney et al., 1997; Thal et al., 2008a,b). In humans Aβ deposits tend to be localized in cortical arteries, arterioles, and capillaries, which show stronger reactivity for Aβ40 (Pantelakis, 1954; Vinters, 1987; Attems et al., 2005). Interestingly, the cerebral vasculature in gorillas was positive for Aβ40 and Aβ42, thioflavine S, X-34, and 6-CN-PiB revealing the fibrillar nature of the Aβ aggregates in the gorilla cerebral vasculature. In addition, Aβ-containing blood vessels were associated with numerous astrocytes indicative of an inflammatory response often associated with neuritic plaques. The histomorphology of Aβ-positive vessels in gorilla are similar to CAA described in squirrel monkeys, indicating a species-specific predilection for CAA rather than parenchymal plaques (Elfenbein et al., 2007). Our findings suggest that Aβ vascular deposition is a widespread phenomenon in aged gorilla brains that contribute to disruption of microcirculation and breakdown of the brain-blood barrier exacerbating Aβ parenchymal pathology in this great ape.

We found that the oldest female gorillas (50 and 55 years old) displayed more widespread neocortical Aβ plaque pathology compared to the youngest female (32 years old) and all male gorillas, suggesting sex-related differences with respect to plaque production. Plaques result from abnormal extracellular aggregation of Aβ40 and Aβ42, two normal byproducts of APP metabolism after sequential cleavage by β- and γ-secretases. The APP amino acid sequence is highly conserved in primates (Martin et al., 1991; Adroer et al., 1997). Both Aβ40 and Aβ42 were found in neocortical and hippocampal plaques as reported in other primates (Walker et al., 1987; Martin et al., 1991; Mufson et al., 1994; Poduri et al., 1994; Gearing et al., 1996, 1997; Kimura et al., 2001; Geula et al., 2002; Lemere et al., 2004, 2008; Bons et al., 2006; Merrill et al., 2011) and nonprimate mammals (Roertgen et al., 1996; Tekirian et al., 1996; Brellou et al., 2005), as opposed to the human condition where the main amylogenic plaque component is the highly fibrillogenic Aβ42. By contrast,

plaques containing Aβ40 were not previously reported in a 44-year-old male western lowland gorilla (Kimura et al., 2001). Although in the current study there were no differences in plaque load between Aβ40 and Aβ42 in the cortical areas examined, Aβ40 displayed a significantly stronger immunoreactivity compared to Aβ42-positive plaques, indicating the predominance of the short and less pathogenic Aβ40 form in gorillas similar to other great apes and some monkeys (Gearing et al., 1996, 1997). The factors underlying species differences between human and nonhuman primates are poorly understood. It is possible that there is a decline in Aβ clearance with age, or there are biophysical differences in the aggregation state of Aβ as well as the longer lifespan of humans that influence the expression of either the short, Aβ40, or long, Aβ42 forms in the parenchyma of human versus nonhuman primates. In the current study, we also showed Aβ oligomers in plaques, which are considered the most toxic Aβ forms affecting synapses and inducing tau phosphorylation (Lacor et al., 2007; Lambert et al., 2007; De Felice et al., 2008).

Plaques in the brains of gorillas were weakly reactive for thioflavine S, 6-CN-PiB (Rosen et al., 2011), β-pleated sheet-specific markers found in neuritic AD plaques. However, plaques strongly stained for X-34, a fluorescence derivative of Congo Red that visualizes all Aβ deposits including diffuse and neuritic plaques as well as cerebrovascular amyloidosis (Ikonomovic et al., 2006). These results confirm findings showing that diffuse rather neuritic/compact plaques are more predominant in the brain of gorillas (Kimura et al., 2001) and other great apes (Gearing et al., 1996, 1997). Conversely, neuritic plaques with swollen neurites, which were not observed in gorillas, have been described in other nonhuman primates (Walker et al., 1987; Poduri et al., 1994; Gearing et al., 1996; Kimura et al., 2003; Lemere et al., 2004, 2008) as well as in human AD (Serrano-Pozo et al., 2011). A number of studies in nonhuman primates have suggested that diffuse plaques (Bons et al., 2006), which have also been described in the brains of cognitively intact elderly people (Mufson et al., 1999; Price et al., 2009) represent an early stage in the AD plaque development, whereas compact/neuritic plaques are associated with late AD stages. Neuritic plaques are associated with deleterious effects on the surrounding neuropil, including an increase in neurite curvature, dystrophic neurites and recruitment of astrocytes, compared to diffuse plaques, which do not trigger these changes in the neuropil (Masliah et al., 1990; Knowles et al., 1999; Lombardo et al., 2003; Vehmas et al., 2003). Staining with SMI-34 revealed a virtual absence of dystrophic neurites and only occasional SMI-34-ir neurons in the neocortex and hippocampus in the oldest female gorilla. Likewise, intact cholinergic fiber geometry in close proximity to Aβ/oligomer plaques lends support to the observation that the aged gorilla brain contains diffuse plaques.

Tau pathology in the aged gorilla

In addition to Aβ plaques, the other pathologic hallmark of AD is the presence of the NFTs. The major constituent of NFTs is the intracellular aberrantly misfolded and abnormally hyperphosphorylated protein tau, a microtubule-stabilizing protein (Binder et al., 2005). We provide the first evidence of tau-positive profiles in the neocortex and hippocampus in western lowland gorillas. Specifically, large numbers of Alz50-positive interneuron-like profiles and fibers, lacking histopathologic abnormalities, were detected in the supragranular layers of the frontal and entorhinal cortex as well as in the hippocampus in all gorillas,

independent of age, suggesting that Alz50 expression is a normal physiological process. However, these neurons were not MC1-positive, a marker for pathological tau, suggesting that they are not at risk to develop AD-like tau pathology. Sections stained for AT8, an early tau phosphorylated epitope (Goedert et al., 1995b) revealed a few scattered positive neurons in the neocortex and hippocampus of the oldest gorillas (present findings). However, previous studies in great apes (Gearing et al., 1997) with the exception of a report in a old chimpanzee which suffered a stroke (Rosen et al., 2008), failed to reveal cytoskeletal tau alterations perhaps due to the lack of the use of a highly specific conformational and phosphorylation-dependent antibodies. Moreover, tau aggregates have also been described in nondiseased or injured nonhuman primate brain (Hartig et al., 2000; Kiatipattanasakul et al., 2000; Schultz et al., 2000; Bons et al., 2006) as well as in nonprimate species (Cork et al., 1988; Braak and Braak, 1991; Nelson et al., 1994; Roertgen et al., 1996). In addition, we also observed scattered Alz50-, MC1-, and AT8-ir cells resembling astrocytic and oligodendrocytic coiled bodies at the boundary of white and gray matter and throughout the cortex in the oldest gorillas. These findings are similar to those described in the aged baboon (Hartig et al., 2000; Schultz et al., 2000) and in longtailed macaques (Kiatipattanasakul et al., 2000; Oyanagi et al., 2001). Conversely, abnormal tau-positive inclusions in glial cells as seen in gorilla are not common in human AD (Ikeda et al., 1998a), which are often seen in other tauopathies without amyloid pathology (e.g., corticobasal degeneration, progressive supranuclear palsy, and amyotrophic lateral sclerosis/parkinsonism-dementia complex of Guam (Ikeda et al., 1998b; Li et al., 1996; Mizutani et al., 1998; Oyanagi et al., 2001). Perhaps the cytoskeletal tau changes that occur during aging in gorillas evolved independent of amyloid-related plaque pathology. Taken together, the present findings confirm and expand the concept that great apes, including gorillas, are vulnerable to tau pathology in advanced aging. However, in contrast to the human brain, this tau phenomenon in aged gorillas is not confined to projection neurons and does not reach the magnitude seen in AD. Perhaps their shorter lifespan prevents the full development of tau pathology seen in more elderly humans. Despite the similarity of tau protein sequence in nonhuman primates and humans (Haase et al., 2004), the interspecies differences in tau histopathology could be a reflection of diverse genetic factors as well as physiological and environmental conditions during primate evolution.

Evolution and AD pathology

The relevance of evolutionary pressure on the development of AD lesions is an area that has received relatively little attention (Rapoport, 1990, 1999; Benzing et al., 1993). In this regard, it appears that AD is a uniquely human disease, as comparable levels of amyloid plaques and intra- or extracellular tau has not been identified in the brain of any natural animal model. The current findings provide evidence that the brains of (very) old gorillas display many of the classic AD pathologic lesions seen in the human condition including extensive amyloid and some tau-bearing profiles. By comparison to amyloid profiles, there are relatively few reports of NFT pathology in nonhuman primates (Cork et al., 1988; Hartig et al., 2000; Schultz et al., 2000) and particularly in great apes (present study; Rosen et al., 2008). Interestingly, the fossil record (Stephan, 1983) and comparative data suggests that the primate brain selectively expanded particularly during hominid evolution (Hill et al., 2010; Sherwood et al., 2012). In AD, NFT pathology is due to phosphorylation and conformational

alterations to the protein tau (Garcia-Sierra et al., 2003). In fact, the evolution of the native structure of tau proteins may partly underlie the interspecies differences in neuronal vulnerability to develop NFTs (Nelson et al., 1996). Recent gene array studies have shown a shift from 3-repeat to 4-repeat tau in NFT-laden human cholinergic basal forebrain neurons in prodromal AD (Ginsberg et al., 2006). It remains to be seen whether a similar shift occurs in the aged great ape brain. Tau sequencing studies have shown both similarities and differences between the structure of this gene in chimpanzees, gorillas, and humans (Holzer et al., 2004). For example, nonhuman primates are homozygous at seven positions for the H2 compared to the H1 haplotype that characterize human tau suggesting that H1, which is the more prevalent of the two haplotypes is human specific and may play a role in developing NFT pathology in AD (Holzer et al., 2004).

The evolutionary mechanism(s) that trigger the vulnerability of telencephalic long projection neurons to form NFTs during the onset of AD are an area of great interest (Morrison and Hof, 1997). It has been speculated that more recently evolved cortical systems are more plastic and are particularly responsive to environmental and to internal factors (Rapoport and Nelson, 2011). It is possible that this neuroplasticity arose from selective alterations in the neuronal cytoskeleton (Di Patre, 1991), the neuropil (Semendeferi et al., 2011; Spocter et al., 2012), microstructure and connections (Krubitzer, 2007; Sherwood et al., 201 1, 2008), as well as epigenetic (Zeng et al., 2012) or microRNA dysregulation during evolution. These factors either individually or together may have played a role in the increase in the neuron-selective vulnerability seen in the human brain and in AD. Hippocampal CA1 projection neurons, which display NFT pathology, demonstrate an increase in the expression of modulators of cytoskeletal reorganization early in disease progression suggestive of regenerative events (Kao et al., 2010). Recently, the human neocortex was shown to exhibit two lateralized frontoparietal cortical networks, which displayed evolutionary expansion, that are not found topologically nor functionally in corresponding macaque monkey cortex (Mantini et al., 2013). It is also possible that amyloid deposits induce physiological demands associated with neuronal plasticity or cell survival. Although Aβ toxicity may influence NFT-like pathology in the aged rhesus monkey cortex (Geula et al., 1998), diffuse and cored amyloid plaques are found in most aged mammalian brains without concomitant NFT pathology (Braak and Braak, 1991; Cork, 1993). Moreover, the neocortical and hippocampal distribution patterns of Aβ and tau pathology in the gorilla were different, suggesting that these lesions develop independently of each other, and amyloid deposition is not a necessary precondition for the formation of NFTs in the aged primate (Schultz et al., 2000) or that there are species differences between human and ape amyloid. Perhaps during hominid evolution alterations in the aggregation of tau occurs within select populations of neurons independent of amyloid. These and other differences between hominoid and other primates require further investigation.

ACKNOWLEDGMENTS

The authors thank Mr. M. Nadeem, Ms. C. Stimpson, Ms. L. Shao, and Ms. S. Shoaga for technical assistance. We also thank Dr. W. Klunk (University of Pittsburgh) for providing X-34 and 6-CN-PiB compounds used in this study.

Grant sponsor: National Science Foundation; Grant numbers: BCS- 0921079 (to M.A.R.) and BCS-0827531 (to C.C.S.); Grant sponsor: James S. McDonnell Foundation; Grant numbers: 22002078 (to C.C.S., P.R.H) and 22002029 (to C.C.S.); Grant sponsor: National Institute of Aging; Grant number: AG14308 (to J.M.E.).

LITERATURE CITED

Adroer R, López-Acedo C, Oliva R. 1997 Conserved elements in the 5' regulatory region of the amyloid precursor protein gene in primates. Neurosci Lett 226:203–206. [PubMed: 9175602]

Arriagada PV, Growdon JH, Hedley-Whyte ET, Hyman BT. 1992 Neurofibrillary tangles but not senile plaques parallel duration and severity of Alzheimer's disease. Neurology 42:631–639. [PubMed: 1549228]

Atsalis S, Margulis S. 2008 Primate reproductive aging: from lemurs to humans. Interdiscipl Top Gerontol 36:186–194.

Attems J, Lintner F, Jellinger KA. 2004 Amyloid beta peptide 1-42 highly correlates with capillary cerebral amyloid angiopathy and Alzheimer disease pathology. Acta Neuropathol 107:283–291. [PubMed: 14986026]

Attems J, Jellinger KA, Lintner F. 2005 Alzheimer's disease pathology influences severity and topographical distribution of cerebral amyloid angiopathy. Acta Neuropathol 110:222–231. [PubMed: 16133541]

Benzing WC, Kordower JH, Mufson EJ. 1993 Galanin immunoreactivity within the primate basal forebrain: evolutionary change between monkeys and apes. J Comp Neurol 336: 31–39. [PubMed: 7504703]

Bierer LM, Hof PR, Purohit DP, Carlin L, Schmeidler J, Davis KL, Perl DP. 1995 Neocortical neurofibrillary tangles correlate with dementia severity in Alzheimer's disease. Arch Neurol 52:81–88. [PubMed: 7826280]

Binder LI, Guillozet-Bongaarts AL, Garcia-Sierra F, Berry RW. 2005 Tau, tangles, and Alzheimer's disease. Biochim Biophys Acta 1739:216–223. [PubMed: 15615640]

Bons N, Rieger F, Prudhomme D, Fisher A, Krause KH. 2006 Microcebus murinus: a useful primate model for human cerebral aging and Alzheimer's disease? Genes Brain Behav 5:120–130. [PubMed: 16507003]

Bouras C, Hof PR, Giannakopoulos P, Michel JP, Morrison JH. 1994 Regional distribution of neurofibrillary tangles and senile plaques in the cerebral cortex of elderly patients: a quantitative evaluation of a one-year autopsy population from a geriatric hospital. Cereb Cortex 4:138–150. [PubMed: 8038565]

Braak H, Braak E. 1991 Neuropathological stageing of Alzheimer-related changes. Acta Neuropathol 82:239–259. [PubMed: 1759558]

Brellou G, Vlemmas I, Lekkas S, Papaioannou N. 2005 Immunohistochemical investigation of amyloid beta-protein (Aβ) in the brain of aged cats. Histol Histopathol 20: 725–731. [PubMed: 15944921]

Brion JP. 1998 Neurofibrillary tangles and Alzheimer's disease. Eur Neurol 40:130–140. [PubMed: 9748670]

Brodmann K 1909 Vergleichende Lokalisationslehre der Grosshirnrinde. Leipzig: Johann Ambrosius Barth.

Bronikowski AM, Altmann J, Brockman DK, Cords M, Fedigan LM, Pusey A, Stoinski T, Morris WF, Strier KB, Alberts SC. 2011 Aging in the natural world: comparative data reveal similar mortality patterns across primates. Science 331:1325–1328. [PubMed: 21393544]

Carmel G, Mager EM, Binder LI, Kuret J. 1996 The structural basis of monoclonal antibody Alz50's selectivity for Alzheimer's disease pathology. J Biol Chem 271:32789–32795. [PubMed: 8955115]

Clifford PM, Siu G, Kosciuk M, Levin EC, Venkataraman V, D'Andrea MR, Nagele RG. 2008 Alpha7 nicotinic acetylcholine receptor expression by vascular smooth muscle cells facilitates the deposition of Aβ peptides and promotes cerebrovascular amyloid angiopathy. Brain Res 1234:158–171. [PubMed: 18708033]

Cork LC. 1993 Plaques in prefrontal cortex of aged, behaviorally-tested rhesus monkeys: incidence, distribution, and relationship to task performance. Neurobiol Aging 14:675–676. [PubMed: 8295684]

Cork LC, Powers RE, Selkoe DJ, Davies P, Geyer JJ, Price DL. 1988 Neurofibrillary tangles and senile plaques in aged bears. J Neuropathol Exp Neurol 47:629–641. [PubMed: 3171607]

De Felice FG, Wu D, Lambert MP, Fernandez SJ, Velasco PT, Lacor PN, Bigio EH, Jerecic J, Acton PJ, Shughrue PJ, Chen-Dodson E, Kinney GG, Klein WL. 2008 Alzheimer's disease-type neuronal tau hyperphosphorylation induced by Aβ oligomers. Neurobiol Aging 29:1334–1347. [PubMed: 17403556]

Di Patre PL. 1991 Cytoskeletal alterations might account for the phylogenetic vulnerability of the human brain to Alzheimer's disease. Med Hypotheses 34:165–170. [PubMed: 2041492]

Doran DM, McNeilage A, Greer D, Bocian C, Mehlman P, Shah N. 2002 Western lowland gorilla diet and resource availability: new evidence, cross-site comparisons, and reflections on indirect sampling methods. Am J Primatol 58: 91–116. [PubMed: 12454955]

Elfenbein HA, Rosen RF, Stephens SL, Switzer RC, Smith Y, Pare J, Mehta PD, Warzok R, Walker LC. 2007 Cerebral beta-amyloid angiopathy in aged squirrel monkeys. Histol Histopathol 22:155–167. [PubMed: 17149688]

Gaillard F, Bonfield S, Gilmour GS, Kuny S, Mema SC, Martin BT, Smale L, Crowder N, Stell WK, Sauvé Y. 2008 Retinal anatomy and visual performance in a diurnal conerich laboratory rodent, the Nile grass rat (*Arvicanthis niloticus*). J Comp Neurol 510:525–538. [PubMed: 18680202]

García-Sierra F, Ghoshal N, Quinn B, Berry RW, Binder LI. 2003 Conformational changes and truncation of tau protein during tangle evolution in Alzheimer's disease. J Alzheimer Dis 5:65–77.

Gearing M, Tigges J, Mori H, Mirra SS. 1996 Aβ40 is a major form of beta-amyloid in nonhuman primates. Neurobiol Aging 17:903–908. [PubMed: 9363802]

Gearing M, Tigges J, Mori H, Mirra SS. 1997 β-Amyloid (Aβ) deposition in the brains of aged orangutans. Neurobiol Aging 18:139–146. [PubMed: 9258890]

Geula C, Wu CK, Saroff D, Lorenzo A, Yuan M, Yankner BA. 1998 Aging renders the brain vulnerable to amyloid beta-protein neurotoxicity. Nat Med 4:827–831. [PubMed: 9662375]

Geula C, Nagykery N, Wu CK. 2002 Amyloid-beta deposits in the cerebral cortex of the aged common marmoset (*Callithrix jacchus*): incidence and chemical composition. Acta Neuropathol 103:48–58. [PubMed: 11837747]

Giannakopoulos P, Herrmann FR, Bussiere T, Bouras C, Kovari E, Perl DP, Morrison JH, Gold G, Hof PR. 2003 Tangle and neuron numbers, but not amyloid load, predict cognitive status in Alzheimer's disease. Neurology 60:1495–1500. [PubMed: 12743238]

Ginsberg SD, Che S, Counts SE, Mufson EJ. 2006 Shift in the ratio of three-repeat tau and four-repeat tau mRNAs in individual cholinergic basal forebrain neurons in mild cognitive impairment and Alzheimer's disease. J Neuro- chem 96:1401–1408.

Goedert M, Jakes R, Spillantini MG, Crowther RA, Cohen P, Vanmechelen E, Probst A, Gotz J, Burki K. 1995a Tau protein in Alzheimer's disease. Biochem Soc Trans 23: 80–85. [PubMed: 7758799]

Goedert M, Jakes R, Vanmechelen E. 1995b Monoclonal antibody AT8 recognises tau protein phosphorylated at both serine 202 and threonine 205. Neurosci Lett 189:167–169. [PubMed: 7624036]

Gomez-Isla T, Price JL, McKeel DW, Jr, Morris JC, Growdon JH, Hyman BT. 1996 Profound loss of layer II entorhinal cortex neurons occurs in very mild Alzheimer's disease. J Neurosci 16:4491–4500. [PubMed: 8699259]

Haase C, Stieler JT, Arendt T, Holzer M. 2004 Pseudophosphorylation of tau protein alters its ability for self-aggregation. J Neurochem 88:1509–1520. [PubMed: 15009652]

Hartig W, Klein C, Brauer K, Schuppel KF, Arendt T, Bruckner G, Bigl V. 2000 Abnormally phosphorylated protein tau in the cortex of aged individuals of various mammalian orders. Acta Neuropathol 100:305–312. [PubMed: 10965801]

Hill J, Inder T, Neil J, Dierker D, Harwell J, Van Essen D. 2010 Similar patterns of cortical expansion during human development and evolution. Proc Natl Acad Sci U S A 107:13135–13140. [PubMed: 20624964]

Hirata-Fukae C, Li HF, Hoe HS, Gray AJ, Minami SS, Hamada K, Niikura T, Hua F, Tsukagoshi-Nagai H, Horikoshi-Sakuraba Y, Mughal M, Rebeck GW, LaFerla FM, Mattson MP, Iwata N, Saido TC, Klein WL, Duff KE, Aisen PS, Matsuoka Y. 2008 Females exhibit more extensive amyloid, but not tau, pathology in an Alzheimer transgenic model. Brain Res 1216:92–103. [PubMed: 18486110]

Holzer M, Craxton M, Jakes R, Arendt T, Goedert M. 2004 Tau gene (MAPT) sequence variation among primates. Gene 341:313–322. [PubMed: 15474313]

Huxley TH. 1863 Evidence as to Man's place in Nature. London: Williams and Norgate.

Ikeda K, Akiyama H, Arai T, Nishimura T. 1998a Glial tau pathology in neurodegenerative diseases: their nature and comparison with neuronal tangles. Neurobiol Aging 19:S85–S91. [PubMed: 9562475]

Ikeda T, Homma Y, Nisida K, Hirase K, Sotozono C, Kinoshita S, Puro DG. 1998b Expression of transforming growth factor-beta s and their receptors by human retinal glial cells. Curr Eye Res 17:546–550. [PubMed: 9617551]

Ikonomovic MD, Abrahamson EE, Isanski BA, Debnath ML, Mathis CA, Dekosky ST, Klunk WE. 2006 X-34 labeling of abnormal protein aggregates during the progression of Alzheimer's disease. Methods Enzymol 412:123–144. [PubMed: 17046656]

Jicha GA, Bowser R, Kazam IG, Davies P. 1997 Alz-50 and MC-1, a new monoclonal antibody raised to paired helical filaments, recognize conformational epitopes on recombinant tau. J Neurosci Res 48:128–132. [PubMed: 9130141]

Jicha GA, Berenfeld B, Davies P. 1999 Sequence requirements for formation of conformational variants of tau similar to those found in Alzheimer's disease. J Neurosci Res 55:713–723. [PubMed: 10220112]

Kao PF, Davis DA, Banigan MG, Vanderburg CR, Seshadri S, Delalle I. 2010 Modulators of cytoskeletal reorganization in CA1 hippocampal neurons show increased expression in patients at mid-stage Alzheimer's disease. PLoS One 5:e13337. [PubMed: 20967212]

Kiatipattanasakul W, Nakayama H, Yongsiri S, Chotiapisitkul S, Nakamura S, Kojima H, Doi K. 2000 Abnormal neuronal and glial argyrophilic fibrillary structures in the brain of an aged albino cynomolgus monkey (*Macaca fascicularis*). Acta Neuropathol 100:580–586. [PubMed: 11045682]

Kim KS, Miller DL, Sapienza VJ, Chen CMJ, Bai C, Grundke-Iqbal I, Currie JR, Wisniewski HM. 1988 Production and characterization of monoclonal antibodies reactive to synthetic cerebrovascular amyloid pepetide. Neurosci Res Commun 2:121–130.

Kimura N, Nakamura S, Goto N, Narushima E, Hara I, Shichiri S, Saitou K, Nose M, Hayashi T, Kawamura S, Yoshikawa Y. 2001 Senile plaques in an aged western lowland gorilla. Exp Anim 50:77–81. [PubMed: 11326427]

Kimura N, Tanemura K, Nakamura S, Takashima A, Ono F, Sakakibara I, Ishii Y, Kyuwa S, Yoshikawa Y. 2003 Age-related changes of Alzheimer's disease-associated proteins in cynomolgus monkey brains. Biochem Biophys Res Commun 310:303–311. [PubMed: 14521910]

Knowles RB, Wyart C, Buldyrev SV, Cruz L, Urbanc B, Hasselmo ME, Stanley HE, Hyman BT. 1999 Plaque-induced neurite abnormalities: implications for disruption of neural networks in Alzheimer's disease. Proc Natl Acad Sci U S A 96:5274–5279. [PubMed: 10220456]

Krubitzer L 2007 The magnificent compromise: cortical field evolution in mammals. Neuron 56:201–208. [PubMed: 17964240]

Lacor PN, Buniel MC, Chang L, Fernandez SJ, Gong Y, Viola KL, Lambert MP, Velasco PT, Bigio EH, Finch CE, Krafft GA, Klein WL. 2004 Synaptic targeting by Alzheimer's-related amyloid beta oligomers. J Neurosci 24:10191–10200. [PubMed: 15537891]

Lacor PN, Buniel MC, Furlow PW, Clemente AS, Velasco PT, Wood M, Viola KL, Klein WL. 2007 Abeta oligomer-induced aberrations in synapse composition, shape, and density provide a molecular basis for loss of connectivity in Alzheimer's disease. J Neurosci 27:796–807. [PubMed: 17251419]

Lambert MP, Velasco PT, Chang L, Viola KL, Fernandez S, Lacor PN, Khuon D, Gong Y, Bigio EH, Shaw P, De Felice FG, Krafft GA, Klein WL. 2007 Monoclonal antibodies that target pathological assemblies of Abeta. J Neuro- chem 100:23–35.

Langergraber KE, Prüfer K, Rowney C, Boesch C, Crockford C, Fawcett K, Inoue E, Inoue-Muruyama M, Mitani JC, Muller MN, Robbins MM, Schubert G, Stoinski TS, Viola B, Watts D, Wittig RM, Wrangham RW, Zuberühler K, Pääbo S, Vigilant L. 2012 Generation times in wild chimpanzees and gorillas suggest earlier divergence times in great ape and human evolution. Proc Natl Acad Sci U S A 109:15716–15721. [PubMed: 22891323]

Lemere CA, Beierschmitt A, Iglesias M, Spooner ET, Bloom JK, Leverone JF, Zheng JB, Seabrook TJ, Louard D, Li D, Selkoe DJ, Palmour RM, Ervin FR. 2004 Alzheimer's disease abeta vaccine reduces central nervous system abeta levels in a non-human primate, the Caribbean vervet. Am J Pathol 165:283–297. [PubMed: 15215183]

Lemere CA, Jiwon Oh, Stantish Heather A., Peng Ying, Pepivani Imelda, Fagan Anne M., Yamaguchi Haruyasu, Westmoreland Susan V., Mansfield Keith G.. 2008 Cerebral amyloid-beta protein accumulation with aging in cottontop tamarins: a model of early Alzheimer's disease? Rejuven Res 11:321–332.

Li F, Iseki E, Kosaka K, Nishimura T, Akiyama H, Kato M. 1996 Progressive supranuclear palsy with frontotemporal atrophy and various tau-positive abnormal structures. Clin Neuropathol 15:319–323. [PubMed: 8937777]

Lombardo JA, Stern EA, McLellan ME, Kajdasz ST, Hickey GA, Bacskai BJ, Hyman BT. 2003 Amyloid-beta antibody treatment leads to rapid normalization of plaque-induced neuritic alterations. J Neurosci 23:10879–10883. [PubMed: 14645482]

Mantini D, Corbetta M, Romani GL, Orban GA, Vanduffel W. 2013 Evolutionarily novel functional networks in the human brain? J Neurosci 33:3259–3275. [PubMed: 23426655]

Martin LJ, Sisodia SS, Koo EH, Cork LC, Dellovade TL, Weidemann A, Beyreuther K, Masters C, Price DL. 1991 Amyloid precursor protein in aged nonhuman primates. Proc Natl Acad Sci U S A 88:1461–1465. [PubMed: 1899927]

Masliah E, Terry RD, Mallory M, Alford M, Hansen LA. 1990 Diffuse plaques do not accentuate synapse loss in Alzheimer's disease. Am J Pathol 137:1293–1297. [PubMed: 2124413]

Merrill DA, Masliah E, Roberts JA, McKay H, Kordower JH, Mufson EJ, Tuszynski MH. 2011 Association of early experience with neurodegeneration in aged primates. Neurobiol Aging 32:151–156. [PubMed: 19321231]

Mizutani T, Inose T, Nakajima S, Kakimi S, Uchigata M, Ikeda K, Gambetti P, Takasu T. 1998 Familial parkinsonism and dementia with ballooned neurons, argyrophilic neuronal inclusions, atypical neurofibrillary tangles, tau-negative astrocytic fibrillary tangles, and Lewy bodies. Acta Neuropathol 95:15–27. [PubMed: 9452818]

Morrison JH, Hof PR. 1997 Life and death of neurons in the aging brain. Science 278:412–419. [PubMed: 9334292]

Mufson EJ, Bothwell M, Hersh LB, Kordower JH. 1989 Nerve growth factor receptor immunoreactive profiles in the normal, aged human basal forebrain: colocalization with cholinergic neurons. J Comp Neurol 285:196–217. [PubMed: 2547849]

Mufson EJ, Benzing WC, Cole GM, Wang H, Emerich DF, Sladek JR, Jr, Morrison JH, Kordower JH. 1994 Apolipo-protein E-immunoreactivity in aged rhesus monkey cortex: colocalization with amyloid plaques. Neurobiol Aging 15:621–627. [PubMed: 7824054]

Mufson EJ, Lavine N, Jaffar S, Kordower JH, Quirion R, Saragovi HU. 1997 Reduction in p140-TrkA receptor protein within the nucleus basalis and cortex in Alzheimer's disease. Exp Neurol 146:91–103. [PubMed: 9225742]

Mufson EJ, Chen EY, Cochran EJ, Beckett LA, Bennett DA, Kordower JH. 1999 Entorhinal cortex beta-amyloid load in individuals with mild cognitive impairment. Exp Neurol 158:469–490. [PubMed: 10415154]

Nagy Z, Esiri MM, Jobst KA, Morris JH, King EM, McDonald B, Litchfield S, Smith A, Barnetson L, Smith AD. 1995 Relative roles of plaques and tangles in the dementia of Alzheimer's disease: correlations using three sets of neuropathological criteria. Dementia 6:21–31. [PubMed: 7728216]

Nakamura S, Nakayama H, Uetsuka K, Sasaki N, Uchida K, Goto N. 1995 Senile plaques in an aged two-humped (Bactrian) camel (*Camelus bactrianus*). Acta Neuropathol 90:415–418. [PubMed: 8546033]

Nelson PT, Greenberg SG, Saper CB. 1994 Neurofibrillary tangles in the cerebral cortex of sheep. Neurosci Lett 170: 187–190. [PubMed: 8041504]

Nelson PT, Stefansson K, Gulcher J, Saper CB. 1996 Molecular evolution of tau protein: implications for Alzheimer's disease. J Neurochem 67:1622–1632. [PubMed: 8858947]

Olichney JM, Ellis RJ, Katzman R, Sabbagh MN, Hansen L. 1997 Types of cerebrovascular lesions associated with severe cerebral amyloid angiopathy in Alzheimer's disease. Ann N Y Acad Sci 826:493–497. [PubMed: 9329731]

Overk CR, Lu PY, Wang YT, Choi J, Shaw JW, Thatcher GR, Mufson EJ. 2012 Effects of aromatase inhibition versus gonadectomy on hippocampal complex amyloid pathology in triple transgenic mice. Neurobiol Dis 45:479–487. [PubMed: 21945538]

Oyanagi K, Tsuchiya K, Yamazaki M, Ikeda K. 2001 Substantia nigra in progressive supranuclear palsy, corticobasal degeneration, and parkinsonism-dementia complex of Guam: specific pathological features. J Neuropathol Exp Neurol 60:393–402. [PubMed: 11305875]

Pantelakis S 1954 [A particular type of senile angiopathy of the central nervous system: congophilic angiopathy, topography and frequency.] Monatsschr Psychiatr Neurol 128:219–256. [PubMed: 13235689]

Perez S, Sendera TJ, Kordower JH, Mufson EJ. 2004 Estrogen receptor alpha containing neurons in the monkey forebrain: lack of association with calcium binding proteins and choline acetyltransferase. Brain Res 1019:55–63. [PubMed: 15306238]

Perez SE, He B, Muhammad N, Oh KJ, Fahnestock M, Ikonomovic MD, Mufson EJ. 2011 Cholinotrophic basal forebrain system alterations in 3xTg-AD transgenic mice. Neurobiol Dis 41:338–352. [PubMed: 20937383]

Perez SE, Getova DP, He B, Counts SE, Geula C, Desire L, Coutadeur S, Peillon H, Ginsberg SD, Mufson EJ. 2012a Rac 1b increases with progressive tau pathology within cholinergic nucleus basalis neurons in Alzheimer's disease. Am J Pathol 180:526–540. [PubMed: 22142809]

Perez SE, Nadeem M, Sadleir KR, Matras J, Kelley CM, Counts SE, Vassar R, Mufson EJ. 2012b Dimebon alters hippocampal amyloid pathology in 3xTg-AD mice. Int J Physiol Pathophysiol Pharmacol 4:115–127. [PubMed: 23071869]

Poduri A, Gearing M, Rebeck GW, Mirra SS, Tigges J, Hyman BT. 1994 Apolipoprotein E4 and beta amyloid in senile plaques and cerebral blood vessels of aged rhesus monkeys. Am J Pathol 144:1183–1187. [PubMed: 8203459]

Price JL, McKeel DW, Jr, Buckles VD, Roe CM, Xiong C, Grundman M, Hansen LA, Petersen RC, Parisi JE, Dickson DW, Smith CD, Davis DG, Schmitt FA, Markesbery WR, Kaye J, Kurlan R, Hulette C, Kurland BF, Higdon R, Kukull W, Morris JC. 2009 Neuropathology of nondemented aging: presumptive evidence for preclinical Alzheimer disease. Neurobiol Aging 30:1026–1036. [PubMed: 19376612]

Raghanti MA, Stimpson CD, Marcinkiewicz JL, Erwin JM, Hof PR, Sherwood CC. 2008 Cholinergic innervation of the frontal cortex: differences among humans, chimpanzees, and macaque monkeys. J Comp Neurol 506:409–424. [PubMed: 18041783]

Rapoport SI. 1990 Integrated phylogeny of the primate brain, with special reference to humans and their diseases. Brain Res Rev 15:267–294. [PubMed: 2289087]

Rapoport SI. 1999 Functional brain imaging in the resting state and during activation in Alzheimer's disease. Implications for disease mechanisms involving oxidative phosphorylation. Ann N Y Acad Sci 893:138–153. [PubMed: 10672235]

Rapoport SI, Nelson PT. 2011 Biomarkers and evolution in Alzheimer disease. Prog Neurobiol. 95:510–513. [PubMed: 21801803]

Rensink AA, de Waal RM, Kremer B, Verbeek MM. 2003 Pathogenesis of cerebral amyloid angiopathy. Brain Res Rev 43:207–223. [PubMed: 14572915]

Roertgen KE, Parisi JE, Clark HB, Barnes DL, O'Brien TD, Johnson KH. 1996 A beta-associated cerebral angiopathy and senile plaques with neurofibrillary tangles and cerebral hemorrhage in an aged wolverine (*Gulo gulo*). Neurobiol Aging 17:243–247. [PubMed: 8744405]

Rosen RF, Farberg AS, Gearing M, Dooyema J, Long PM, Anderson DC, Davis-Turak J, Coppola G, Geschwind DH, Pare JF, Duong TQ, Hopkins WD, Preuss TM, Walker LC. 2008 Tauopathy with

paired helical filaments in an aged chimpanzee. J Comp Neurol 509:259–270. [PubMed: 18481275]

Rosen RF, Walker LC, Levine H, 3rd. 2011 PIB binding in aged primate brain: enrichment of high-affinity sites in humans with Alzheimer's disease. Neurobiol Aging 32: 223–234. [PubMed: 19329226]

Rosene DL, Van Hoesen GW. 1987 The hippocampal formation of the primate brain: a review of some comparative aspects of cytoarchitecture and connections In: Jones EG, Peters A, editors. Cerebral cortex. Further aspects of cortical function, including hippocampus. New York: Plenum Press, p 345–456.

Scally A, Dutheil JY, Hillier LW, Jordan GE, Goodhead I, Herrero J, Hobolth A, Lappalainen T, Mailund T, Marques- Bonet T, McCarthy S, Montgomery SH, Schwalie PC, Tang YA, Ward MC, Xue Y, Yngvadottir B, Alkan C, Andersen LN, Ayub Q, Ball EV, Beal K, Bradley BJ, Chen Y, Clee CM, Fitzgerald S, Graves TA, Gu Y, Heath P, Heger A, Karakoc E, Kolb-Kokocinski A, Laird GK, Lunter G, Meader S, Mort M, Mullikin JC, Munch K, O'Connor TD, Phillips AD, Prado-Martinez J, Rogers AS, Sajjadian S, Schmidt D, Shaw K, Simpson JT, Stenson PD, Turner DJ, Vigilant L, Vilella AJ, Whitener W, Zhu B, Cooper DN, de Jong P, Dermitzakis ET, Eichler EE, Flicek P, Goldman N, Mundy NI, Ning Z, Odom DT, Ponting CP, Quail MA, Ryder OA, Searle SM, Warren WC, Wilson RK, Schierup MH, Rogers J, Tyler-Smith C, Durbin R. 2012 Insights into hominid evolution from the gorilla genome sequence. Nature 483:169–175. [PubMed: 22398555]

Schultz C, Dehghani F, Hubbard GB, Thal DR, Struckhoff G, Braak E, Braak H. 2000 Filamentous tau pathology in nerve cells, astrocytes, and oligodendrocytes of aged baboons. J Neuropathol Exp Neurol 59:39–52. [PubMed: 10744034]

Selkoe DJ. 2000 The origins of Alzheimer disease: A is for amyloid. JAMA 283:1615–1617. [PubMed: 10735401]

Selkoe DJ. 2001 Alzheimer's disease: genes, proteins, and therapy. Physiol Rev 81:741–766. [PubMed: 11274343]

Semendeferi K, Teffer K, Buxhoeveden DP, Park MS, Bludau S, Amunts K, Travis K, Buckwalter J. 2011 Spatial organization of neurons in the frontal pole sets humans apart from great apes. Cereb Cortex 21:1485–1497. [PubMed: 21098620]

Serrano-Pozo A, Frosch MP, Masliah E, Hyman BT. 2011 Neuropathological alterations in Alzheimer disease. Cold Spring Harbor Perspect Med 1:a006189.

Sherwood CC, Subiaul F, Zawidzki TW. 2008 A natural history of the human mind: tracing evolutionary changes in brain and cognition. J Anat 212:426–454. [PubMed: 18380864]

Sherwood CC, Gordon AD, Allen JS, Phillips KA, Erwin JM, Hof PR, Hopkins WD. 2011 Aging of the cerebral cortex differs between humans and chimpanzees. Proc Natl Acad Sci U S A 108:13029–13034. [PubMed: 21788499]

Sherwood CC, Bauernfeind AL, Bianchi S, Raghanti MA, Hof PR. 2012 Human brain evolution writ large and small. Prog Brain Res 195:237–254. [PubMed: 22230630]

Spocter MA, Hopkins WD, Barks SK, Bianchi S, Hehmeyer AE, Anderson SM, Stimpson CD, Fobbs AJ, Hof PR, Sherwood CC. 2012 Neuropil distribution in the cerebral cortex differs between humans and chimpanzees. J Comp Neurol 20:2917–2929.

Stephan H 1983 Evolutionary trends in limbic structures. Neurosci Biobehav Rev 7:367–374. [PubMed: 6669324]

Styren SD, Hamilton RL, Styren GC, Klunk WE. 2000 X-34, a fluorescent derivative of Congo Red: a novel histochemical stain for Alzheimer's disease pathology. J Histochem Cytochem 48:1223–1232. [PubMed: 10950879]

Tekirian TL, Cole GM, Russell MJ, Yang F, Wekstein DR, Patel E, Snowdon DA, Markesbery WR, Geddes JW. 1996 Car- boxy terminal of beta-amyloid deposits in aged human, canine, and polar bear brains. Neurobiol Aging 17:249–257. [PubMed: 8744406]

Thal DR, Griffin WS, Braak H. 2008a Parenchymal and vascular Abeta-deposition and its effects on the degeneration of neurons and cognition in Alzheimer's disease. J Cell Mol Med 12:1848–1862. [PubMed: 18624777]

Thal DR, Griffin WS, de Vos RA, Ghebremedhin E. 2008b Cerebral amyloid angiopathy and its relationship to Alzheimer's disease. Acta Neuropathol 1 15:599–609.

Vehmas AK, Kawas CH, Stewart WF, Troncoso JC. 2003 Immune reactive cells in senile plaques and cognitive decline in Alzheimer's disease. Neurobiol Aging 24:321–331. [PubMed: 12498966]

Vickers JC, Riederer BM, Marugg RA, Buíe-Scherrer V, Buíe L, Delacourte A, Morrison JH. 1994 Alterations in neurofilament protein immunoreactivity in human hippocampal neurons related to normal aging and Alzheimer's disease. Neuroscience 62:1–13. [PubMed: 7816192]

Vinters HV. 1987 Cerebral amyloid angiopathy. A critical review. Stroke 18:311–324. [PubMed: 3551211]

Walker LC, Masters C, Beyreuther K, Price DL. 1990 Amyloid in the brains of aged squirrel monkeys. Acta Neuropathol 80:381–387 [PubMed: 2239150]

Walker LC, Kitt CA, Schwam E, Buckwald B, Garcia F, Sepinwall J, Price DL. 1987 Senile plaques in aged squirrel monkeys. Neurobiol Aging 8:291–296. [PubMed: 3306432]

Wolozin BL, Pruchnicki A, Dickson DW, Davies P. 1986 A neuronal antigen in the brains of Alzheimer patients. Science 232:648–650. [PubMed: 3083509]

Youmans KL, Tai LM, Kanekiyo T, Stine WB, Jr, Michon SC, Nwabuisi-Heath E, Manelli AM, Fu Y, Riordan S, Eimer WA, Binder L, Bu G, Yu C, Hartley DM, LaDu MJ. 2012 Intraneuronal Abeta detection in 5xFAD mice by a new β-specific antibody. Mol Neurodegen 7:8.

Younkin SG. 1998 The role of Aβ42 in Alzheimer's disease. J Physiol (Paris) 92:289–292. [PubMed: 9789825]

Zeng J, Konopka G, Hunt BG, Preuss TM, Geschwind D, Yi SV. 2012 Divergent whole-genome methylation maps of human and chimpanzee brains reveal epigenetic basis of human regulatory evolution. Am J Hum Genet 91:455–465. [PubMed: 22922032]

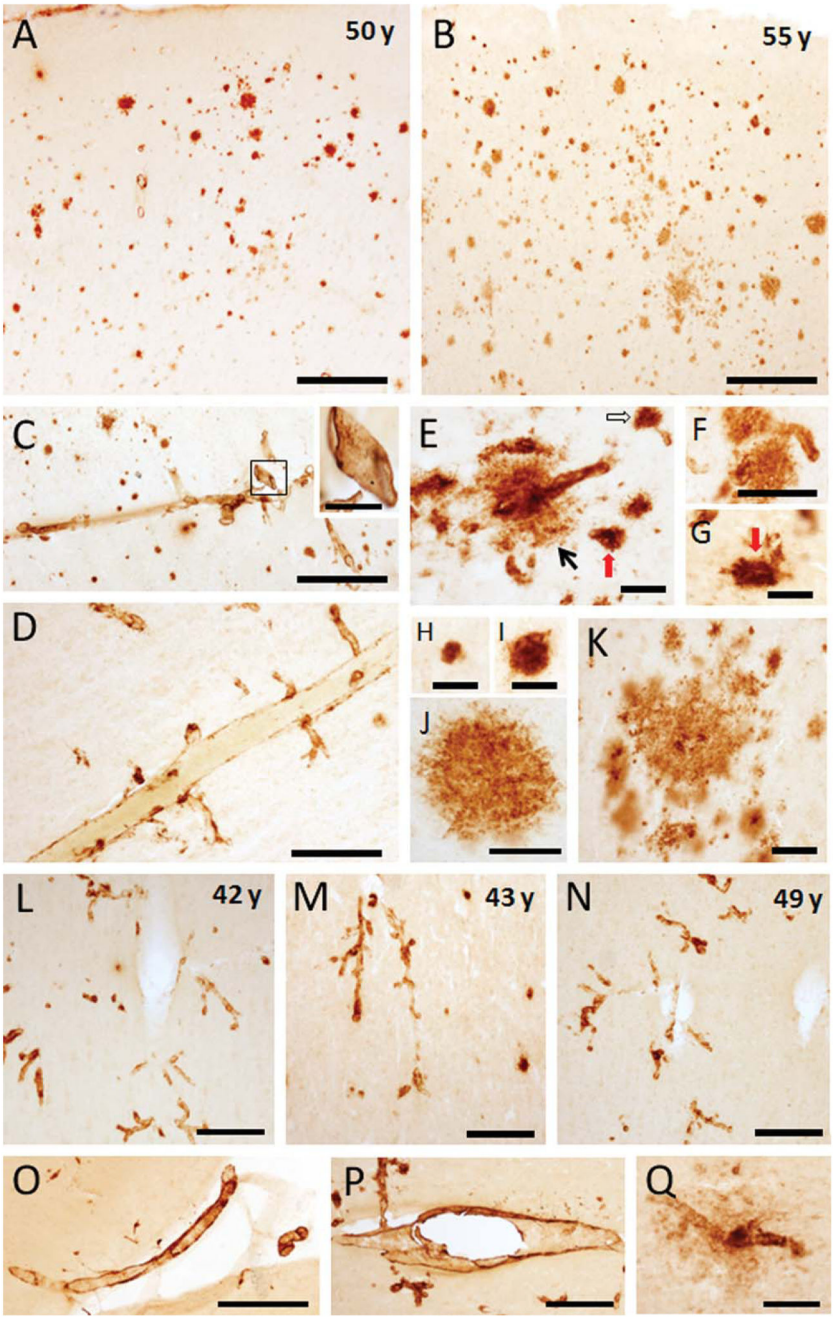

Figure 1.

Photomicrographs showing APP/Aβ-ir plaques in the frontal cortex (area 8) in 50- (**A**) and 55-year-old female gorillas (**B**). Note that the older gorilla displayed many more neocortical plaques than the younger. **C–G**. Images showing different size APP/Aβ-ir blood vessels in the same animals, including meningeal vessels branching into the neocortex (C,D), arterioles with Aβ leakage (E) (black arrow), discrete capillaries, or associated with plaques (unfilled arrow in E) and collapsed capillaries (E,G) (red arrows). Inset shows a high magnification of a meningeal positive blood vessel outlined in panel C. High-power images showing different sizes and morphologies of APP/Aβ-ir plaques in a 55-year-old gorilla: small plaques (**H,I**),

larger plaques with amorphous outline (**J**), and clusters of plaques (**K**). Photomicrographs illustrating the presence of APP/Aβ-positive blood vessels compared to a lack of neocortical plaques in 42- (**L**), 43- (**M**), and 49- (**N**)-year-old male gorillas. **O,P:**. Images showing APP/Aβ-positive meningeal and parenchymal blood vessels in 49- and 42-year-old male gorillas, respectively. **Q:** Image of a neocortical capillary surrounded by amyloid in a 49-year-old male gorilla. Scale bars = 500 μm in A-C,O,P; 200 μm in D,L-N; 100 μm in F,Q and inset in C; 50 μm in E,G,J,K; 25 μm in H,I.

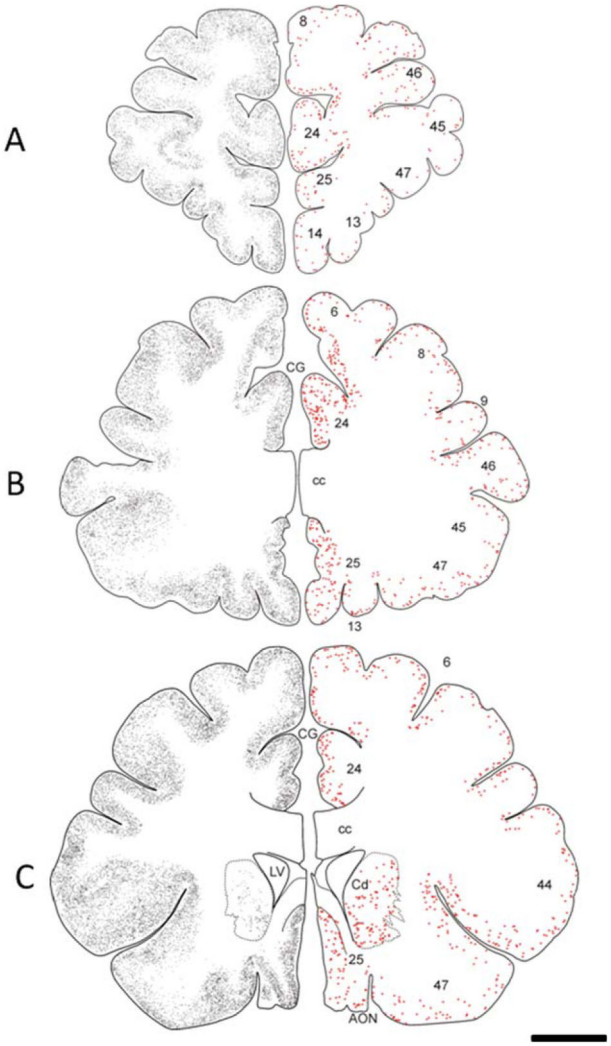

Figure 2.

Schematic drawings of the frontal cortex of a 55-year-old female gorilla representing the rostral to caudal distribution of APP/Aβ-ir plaques (gray small dots) and Alz50-ir neurons (red dots) AON, anterior olfactory nucleus; Cd, caudate nucleus; CG, cingulate gyrus; cc, corpus callosum; LV, lateral ventricle. Scale bar = 1 cm.

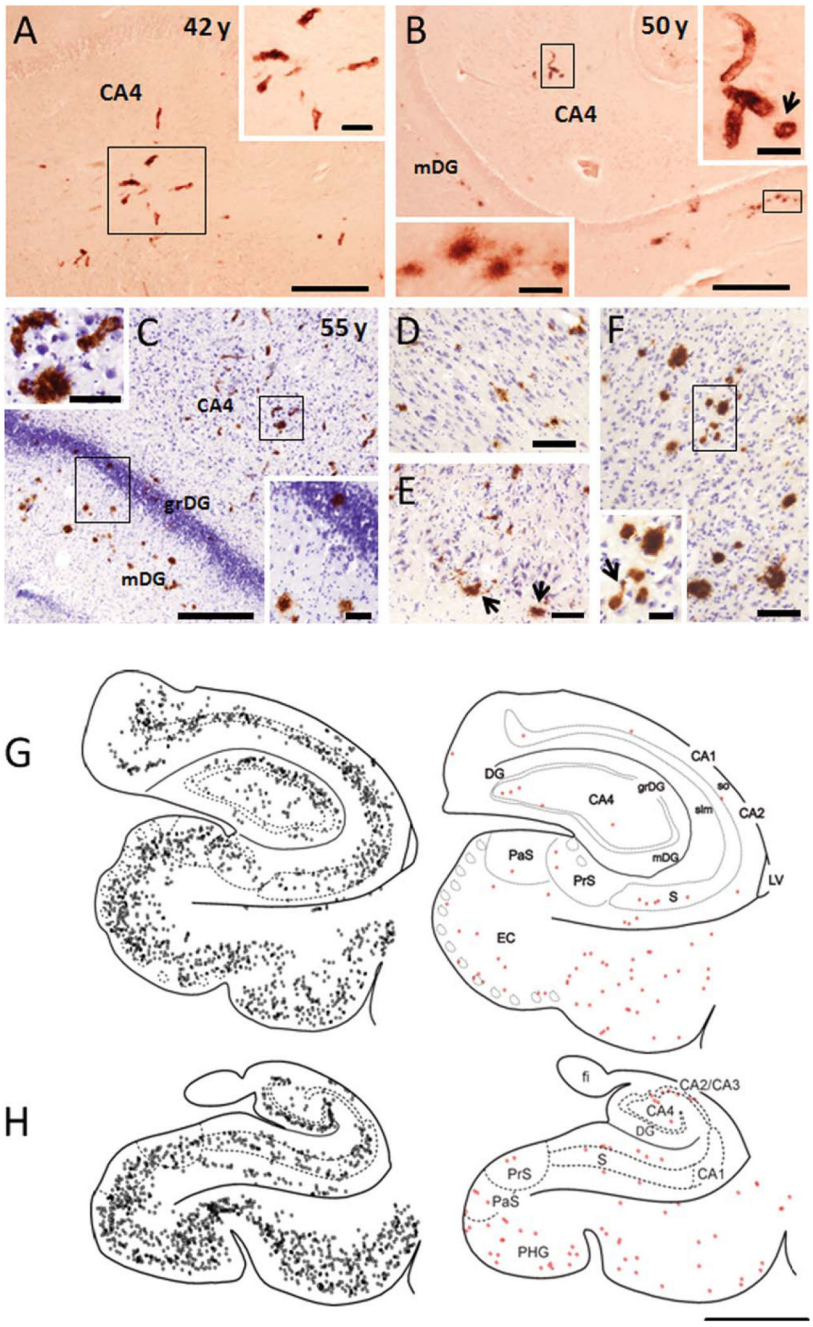

Figure 3.

Photomicrographs showing APP/Aβ-ir blood vessels and plaques in the hippocampal CA4 field and dentate gyrus in a 42-year-old male (**A**) as well as in a 50- (**B**), and 55- (**C**) year-old female gorilla. Insets show high-power images of labeled capillaries (A–C), a collapsed capillary (arrow, B), and plaques within the molecular (B,C) and granule cell layer of the dentate gyrus (C), as outlined in A–C. Note the presence of many more plaques in the molecular and granular layers of the dentate gyrus of a 55-year-old gorilla. **D–F**. Images showing APP/Aβ-ir plaques in the hippocampal CA1 pyramidal cell layer (D), entorhinal cortex (E), and parahippocampal gyrus (F) in a 55-year-old female gorilla. Note the presence

of plaques in the layer II islands (arrows) of the entorhinal cortex. Inset in F shows a high-power image of Aβ-positive plaques and capillary (arrow) as outlined in panels **F–H**. Schematic drawings showing the rostrocaudal distribution of APP/Aβ-ir plaques (gray squares) and Alz50-ir profiles (red squares) in the hippocampus of a 55-year-old gorilla. CA1, CA2, CA3 fields CA2, CA3 of the hippocampus; CA4, hilar portion of the CA3 of the hippocampus; DG, dentate gyrus; EC, entorhinal cortex; fi, fimbria; grDG, granular layer of dentate gyrus; LV, lateral ventricle; mDG, molecular layer of the dentate gyrus; PaS, parasubiculum; PHG, parahippocampal gyrus; PrS, presubiculum; S, subiculum; slm, stratum lacunosum-moleculare of the hippocampus; so, stratum oriens of the hippocampus. Scale bars = 0.500 cm in G,H; 500 μm in A–C; 200 μm in D; 100 μm in E,F and insets in A,C; 50 μm insets in B; 25 μm inset in F.

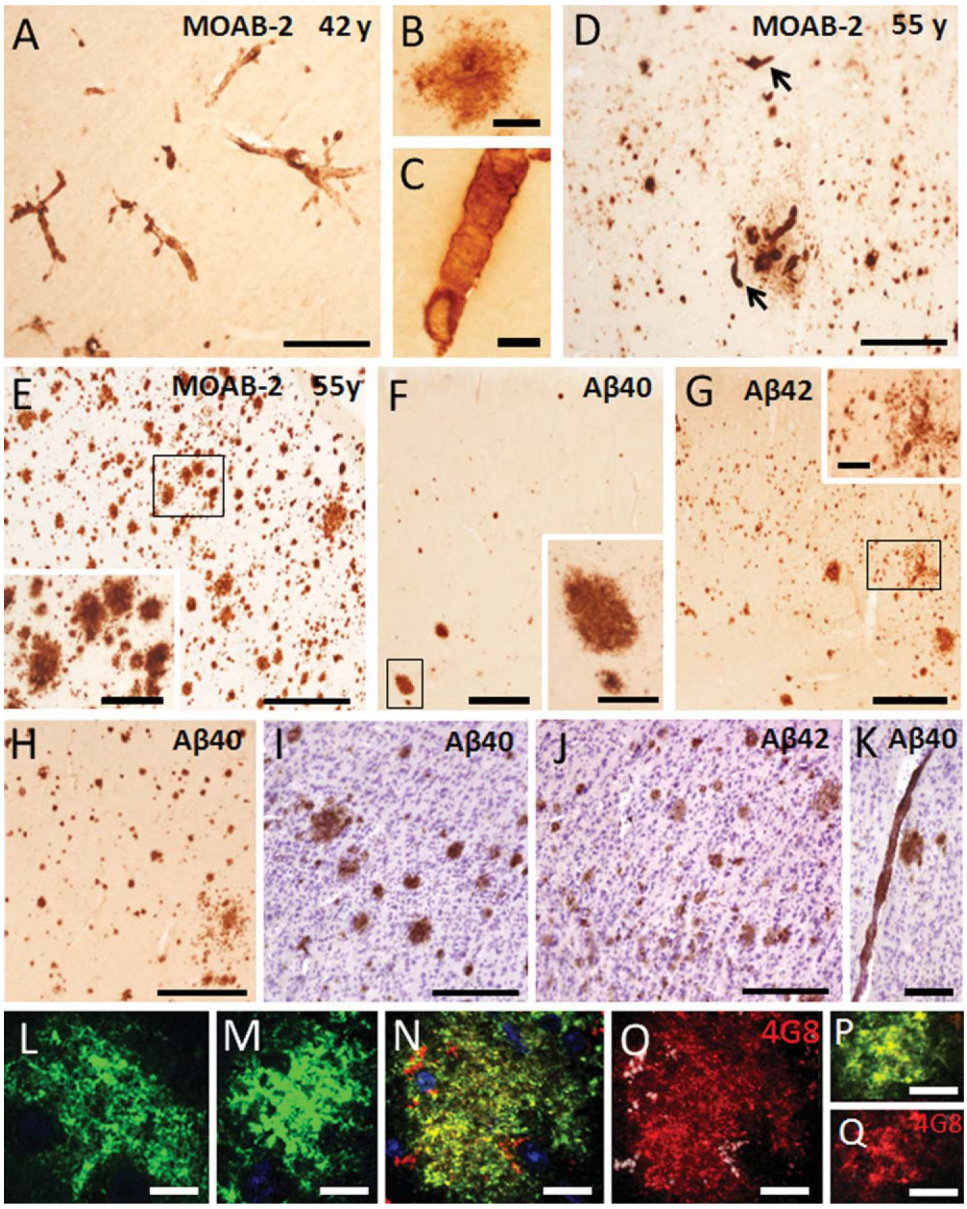

Figure 4.

A: Photomicrograph showing blood vessels stained with the Aβ pan-marker MOAB-2 in the neocortex of a 42-year-old male gorilla. High-power photomicrographs showing an MOAB-2-ir plaque **(B)** and an MOAB-2-ir blood vessel **(C)** in a 42-year-old male gorilla. **D,E:** Photomicrographs showing MOAB-ir plaques and/or blood vessels (arrows) in Brodmann cortical areas 6 and 8, respectively, in a 55-year-old gorilla. The inset shows high-power image of MOAB-2-positive plaques from the boxed area in panel E. **F,G:** Images illustrating differences in the pattern of staining for Aβ40 and Aβ42 in adjacent sections of area 24 in a 55-year-old gorilla, respectively. Note many more small Aβ42ir plaques compared to Aβ40-positive plaques. Insets show high-power images of plaques from the boxed areas in panels F,G. **H**. Image illustrating numerous Aβ40-ir plaques in the orbitofrontal cortex (area 13) of a 55-year-old female. Photomicrographs showing difference

in Aβ40 **(I)** and Aβ42 **(J)** cortical plaque intensity found in a 55-year-old female gorilla. Note the Aβ40-positive plaques show a stronger immunoreactivity compared to Aβ42-ir plaques. Aβ40-ir blood vessel found in the cortex of a 55-year-old gorilla **(K)**. Tissue counterstained with cresyl violet to reveal cytoarchitecture (I–K). Confocal images showing an Aβ oligomeric positive plaque (green) seen in the frontal cortex of a 55-year-old gorilla (**L)** and late stage human AD **(M)**. Confocal images showing double labeling for Aβ oligomers (NU4) and APP/Aβ (4G8) (yellow) (**N,P**) in a plaque as well as single staining for APP/Aβ (red) (**O,Q**) in the neocortex of 55-year-old gorilla (N,O) compared to tissue from a human AD case (P,Q). DAPI (blue) nuclear staining in N. Scale bars = 500 μm in E,G,H; 300 μm in A,D,F and inset in E; 200 μm in I–J; 150 μm in K; 100 μm in inset in G; 50 μm in B,C; 10 μm in L–Q.

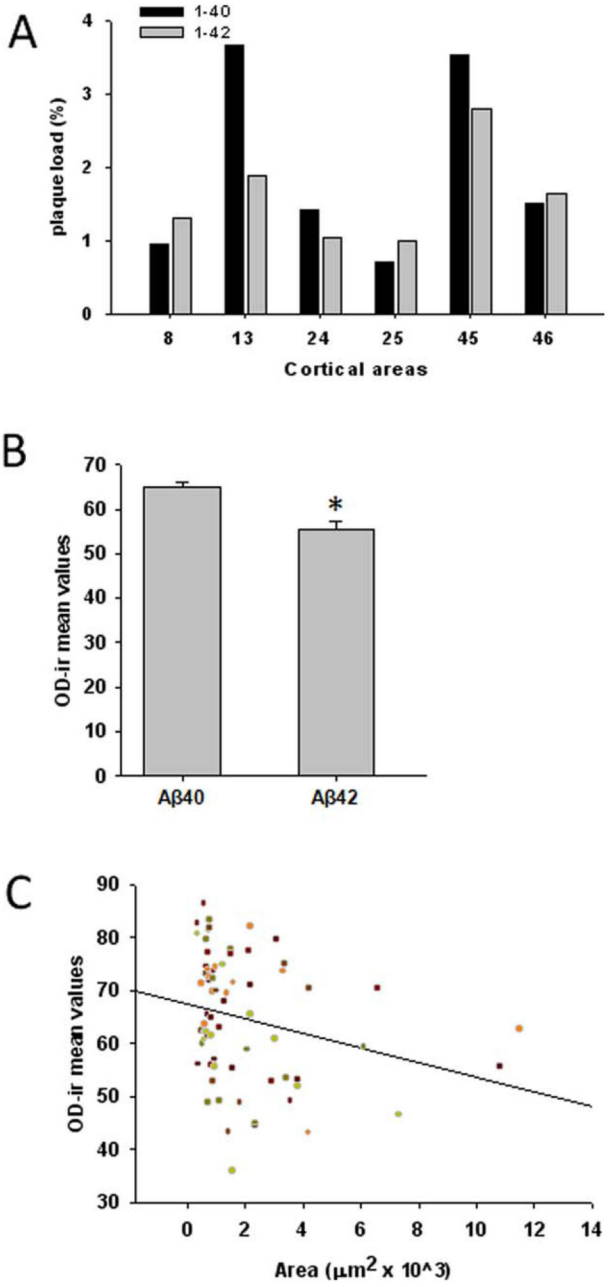

Figure 5.

A: Histogram showing plaque load (%) mean values for Aβ40 and Aβ42 in the different cortical areas obtained at levels depicted in Figure 2A from a 55-year-old gorilla. **B:** Analysis of Aβ40 and Aβ42 optical density (OD) mean value revealed Aβ40 immunoreactivity in plaques was significantly stronger than Aβ42. **C.** Linear regression analysis of Aβ40 OD measurements and plaque area (μm^2) revealed that plaque size correlated negatively with OD measurements for Aβ40. [Color figure can be viewed in the online issue, which is available at wileyonlinelibrary.com.]

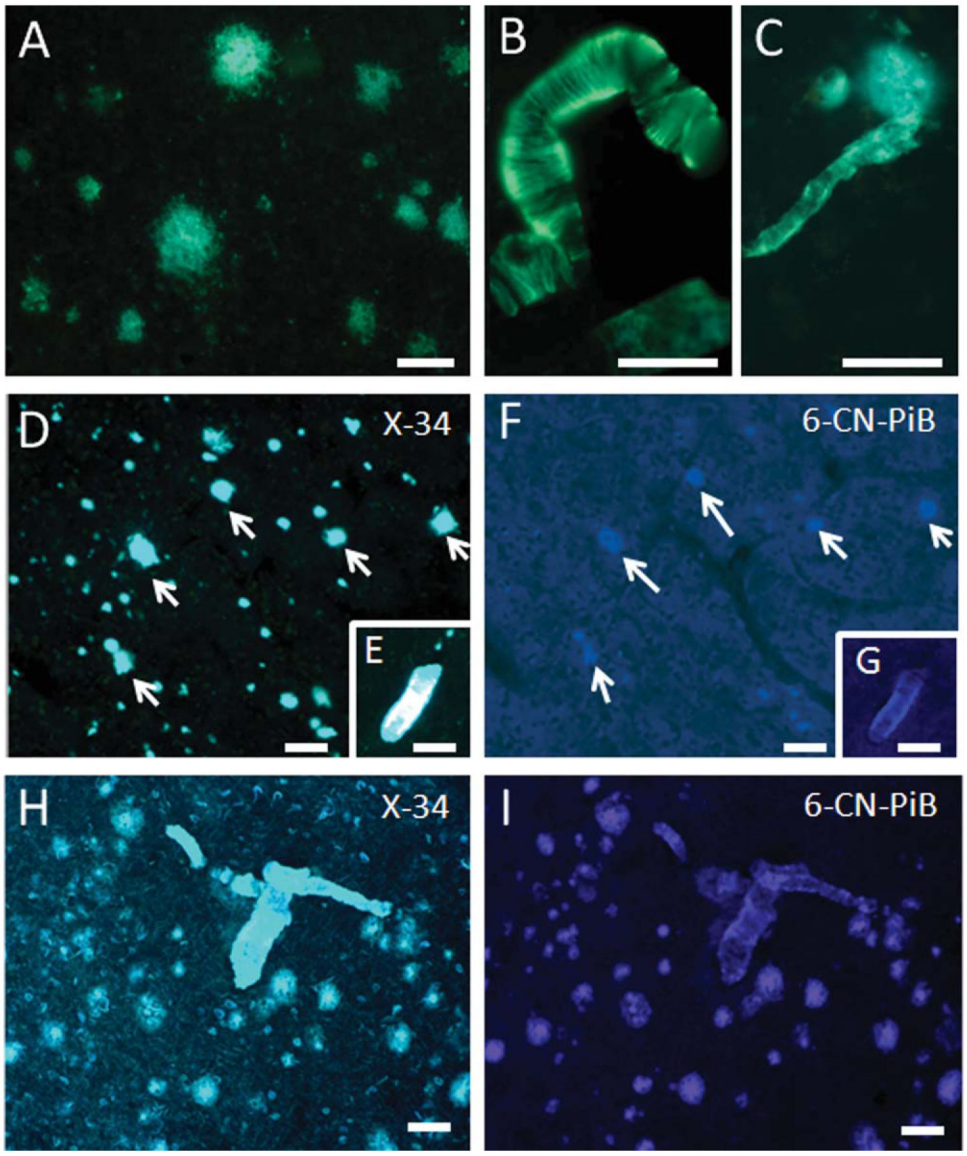

Figure 6.

Photomicrographs showing thioflavine S-positive plaques (**A**), meningeal blood vessels (**B**), and capillaries (**C**) in a 55-year-old female gorilla. Note the stronger thioflavine S staining of blood vessels compared to plaques. Images showing numerous X-34-positive plaques (**D**) in the 55-year-old female gorilla neocortex, compared to a few weakly 6-CN-PIB-positive plaques (**F**). Photomicrographs showing reactive microvessels stained for X-34 (**E**) and 6-CN-PIB (**G**) in the frontal cortex of a 55-year-old female gorilla. **H,I:** Photos showing correspondence between plaques and blood vessels stained with X-34 and 6-CN-PIB in human AD. Scale bars = 100 μm in B,D,F,H,I; 80 μm in A; 50 μm in C,E,G.

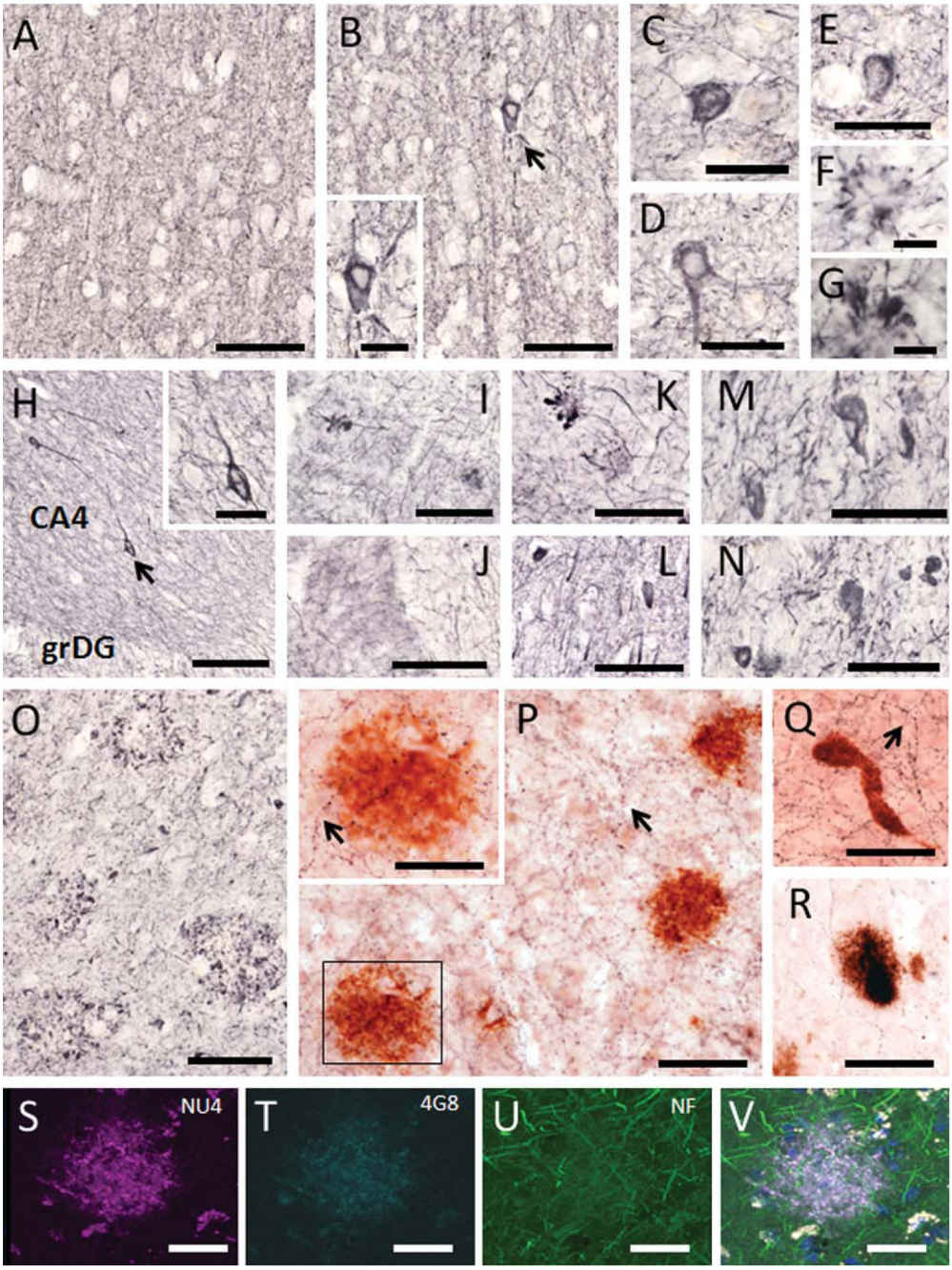

Figure 7.

Photomicrographs showing SMI-34-ir neurites (**A,B,F,G**) and cells (**C–E**) found in the frontal cortex of a 42-year-old male (A) and a 55-year-old female (B–G) gorilla. Inset shows a high-power image of the SMI-34 neuron shown in panel B (arrow). Note the absence of SMI-34 dystrophic processes or cells in a 42-year-old male gorilla, whereas SMI-34-ir cells (with NFT-like appearance) (C–E) and swollen dystrophic neurites (F,G) were found in the cortex of the 55-year-old female gorilla. **H:** Image of the dentate gyrus and hilar portion of the CA3 hippocampal field illustrating SMI-34-ir neurites and cells in a 55-year-old gorilla.

Inset shows a detail of the neuron shown in panel H (arrow). **I–L:** Images exhibiting the presence of swollen SMI-34-ir dystrophic neurites in the molecular layer of the dentate gyrus (I), subiculum (K) as well as SMI-34-ir cells in the subiculum (L) in a 55-year-old gorilla. Dystrophic profiles were not found in the dentate gyrus of a 42-year-old male gorilla (J). Photomicrographs showing SMI-34-ir neurons (**M,N**), neuropil threads (**M–O**), and clusters of swollen dystrophic neurites (O) found in the human AD cortex. Sections dual labeled showing numerous fine ChAT-ir fibers (blue; arrows) with normal morphology adjacent to APP/Aβ-positive plaques (red; **P,R**) and a microvessel (**Q**) in the frontal cortex (P,Q) and dentate gyrus (R) in the 55-year-old female gorilla. Inset shows a high-power image from the boxed area in panel P showing ChAT-ir fibers passing throughout the plaque (red) without signs of dystrophy. Confocal immunofluorescence single-labeled images showing Aβ oligomers (NU4, magenta; **S**), APP/Aβ (4G8, cyan; **T**), neurofilament proteins (NF, green; **U**), and the merged image (light purple; **V**) in a neocortical plaque from a 55-year-old gorilla. Note the absence of neuritic dystrophy within the plaque. Nuclear staining (DAPI) in V is blue. CA4, hilar portion of the CA3 field of the hippocampus; grDG, granular cell layer of the dentate gyrus. Scale bars = 100 μm in A,B,H,I–L,O,P,Q; 50 μm in C–E,M,N, and insets in P,H; 30 μm in R–V; 25 μm in F,G and inset in B.

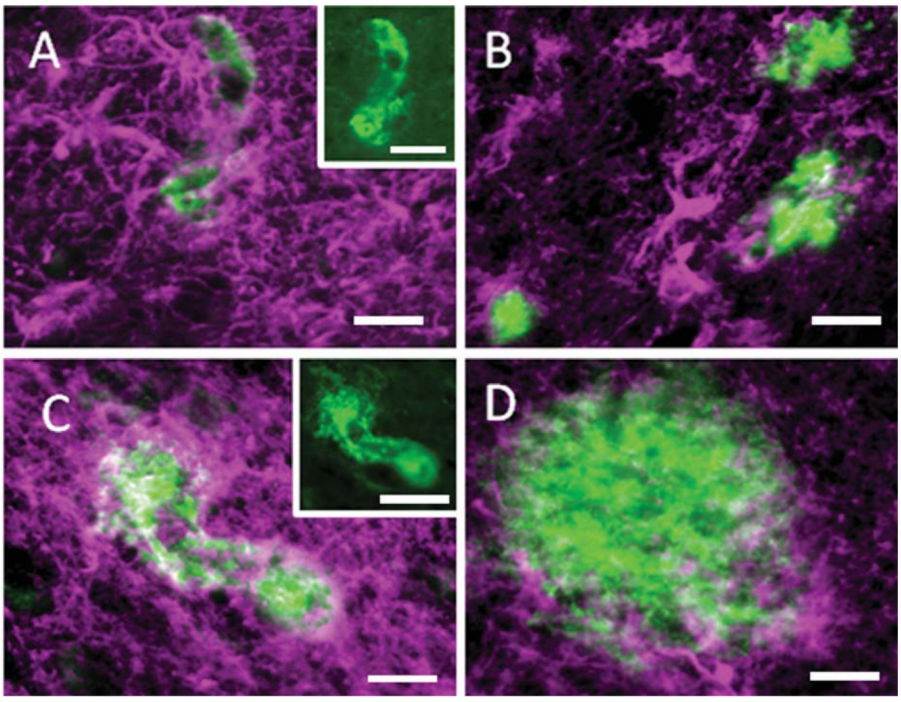

Figure 8.

Immunofluorescence images showing GFAP-positive astrocytes (magenta) adjacent to APP/Aβ-positive (green) capillaries (**A,C**) and plaques (**B,D**) in the hippocampus of a 55-year-old female gorilla. Insets show single immunostained images of APP/Aβ-ir microvessels from panels A and B, respectively. Note the stronger GFAP immunoreactivity next to the vessels compared to the plaques. Scale bars = 25 μm in A–D; 50 μm insets in A,C.

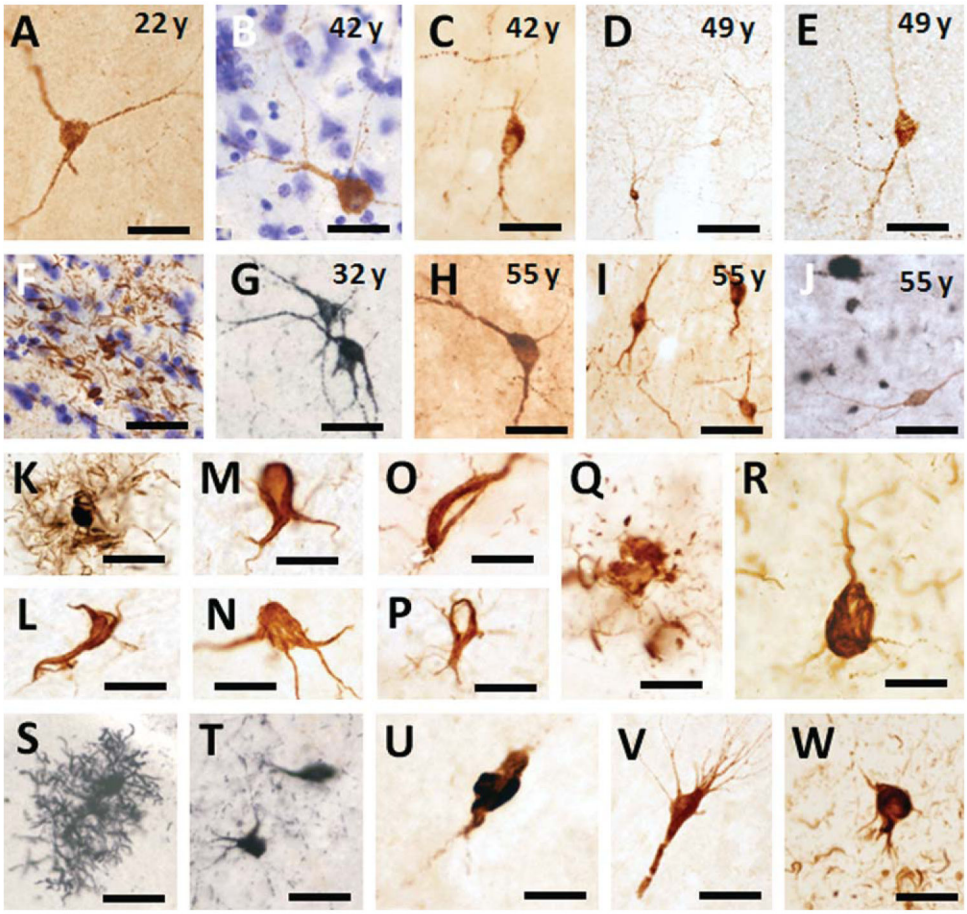

Figure 9.

Photomicrographs showing Alz50-ir interneurons (**A–E,G–I**), fibers (D), clusters of neurites (**F**) in frontal (A–C,E,F), temporal (C,H), and subicular cortex (I) in male (A–F) and female (**G–J**) gorillas across the age range. J: Dual immunolabeled showing cortical Alz50-ir neurons (brown) in close proximity of APP/Aβ (6E10)-positive plaques (black) with no evident morphological alterations in a 55-year-old female gorilla. Tissue in panels B,F was counterstained with cresyl violet. **K–M**. Photomicrographs showing astrocytic Alz50-ir (K) and oligodendrocytic coiled profiles (L,M) found in the neocortex of a 49-year-old male gorilla. Cortical Alz50-ir oligodendrocytic coiled profile from a 50-year-old female gorilla (**N**). MC1-ir oligodendrocytic coiled profiles (**O,P**) and dystrophic neurite clusters (**Q**) in the neocortex of a 49-year-old male gorilla. Alz50-positive neuron found in AD frontal cortex (**R**). Astrocytic AT8-ir profile in the frontal cortex of a 55-year-old female gorilla (**S**). AT8-ir neurons in the neocortex (**T**), subiculum (**U**), and hippocampal CA1 pyramidal cell layer (**V**) in a 55-year-old female gorilla. **W:** Image of an AT8-ir NFT and neuropil threads in the frontal cortex of an AD subject. Scale bars = 100 μm in D; 50 μm in A,C,E,I-K,S,T,V,W; 30 μm in G,H,R; 25 μm in B,F,L-Q,U.

TABLE 1.

Gorilla Specimens and Available Tissue

ID	Age	Sex	Frontal cortex	Hippocampus
H	32	F	√[1]	√
S	35	F	n/a	√
G	50	F	√	√
J	55	F	√	√
JB	13	M	n/a	√
B	22	M	√	n/a
W	42	M	√	√
M	43	M	√	n/a
R	49	M	√	n/a

[1]Few sections. n/a not available.

TABLE 2.

Summary of Antibodies Used

Antigen	Antibodies	Dilution	Company and cat. #
APP/Aβ (6E10)	Mouse monoclonal to residues 1–16 of Aβ (DAEFRHDSGYEVHHQK)	1:1,000	Covance; # SIG-39320
APP/Aβ (4G8)	Mouse monoclonal to residues 17–24 of Aβ (LVFFAEDV)	1:1,000	Covance; # SIG-39220
Aβ (MOAB-2)	Mouse monoclonal to Aβ	1:600	Gift from M. J. LaDu
Aβ40	Rabbit polyclonal to C teminus of human Aβ40 (LMVGGVV)	1:100	Millipore; # AB5074P
Aβ42	Rabbit polyclonal to C terminus of human Aβ A4 protein	1:100	Invitrogen; # 700254
Aβ oligomers (NU4)	Mouse monoclonal to Aβ-derived diffusible ligands	1:2,000	Gift from W. Klein
Tau (Alz50)	Mouse monoclonal to tau residues 5–15 (QEFEVMEDHA), 312–322 (GSTENLKHQPGG)	1:500	Gift from P. Davies
Tau (MC1)	Mouse monoclonal to tau residues 5–15 (QEFEVMEDHA), 312–322 (GSTENLKHQPGG)	1:200	Gift from P. Davies
Tau (AT8)	Mouse monoclonal to tau phospoSerine 202 and phosphoThreonine 205	1:1,000	ThermoFisher; # MN1020
ChAT	Goat polyclonal to choline acetyltransferase	1:1,000	Millipore; # AB144P
SMI-34	Mouse monoclonal to phosphorylated 200 kDa and 160 kDa neurofilaments	1:1,000	Abcam; # 24571
Neurofilaments	Rabbit polyclonal to whole neuron(Neuro-Chrom Pan Neuronal Marker)	1:1,000	Millipore; # MAB2300A4
GFAP	Rabbit polyclonal to glial fibrillary acidic protein	1:400	Dako; # Z0334